5. Formulation development and Evaluation of Nanoemulsion

5.1 Introduction

The aim of this study was to formulate and assess innovative nanoemulsions containing Luliconazole and Tavaborole for dermal application. Nanoemulsions are known for their ability to enhance the penetration of drugs into the skin, owing to their high capacity for dissolving lipophilic substances, extensive surface area, close contact with skin, and inherent ability to facilitate drug transport through the stratum corneum due to their oil and surfactant content (1-3). Various therapeutic agents have been incorporated into nanoemulsions to boost drug delivery through the skin and nails (4-10). A systematic approach based on Quality by Design (QbD) principles, incorporating statistical experimental designs, was adopted to thoroughly investigate how different materials and process variables influence the key attributes of the formulation (11, 12).

5.2 Materials and Instruments

Table 5.1 List of Materials

Chemical/Reagent	Manufacturer/Supplier
Luliconazole	Sun Pharmaceutical Industries Ltd., Vadodara
Tavaborole	Symed labs limited, Hyderabad
Methanol (A.R & HPLC grade)	Spectrochem Pvt. Ltd., Mumbai
Capmul MCM C8	Abitec Corporation, USA
Coconut Oil	Marico India Pvt. Ltd., Mumbai
Cremophore EL	Sigma Aldrich, India
Pluronic F 127	Sigma Aldrich, India
Distilled water	Prepared in house
Carbopol 974 P	Lubrizol, India
Propylene glycol	Astron Pharmaceutical Pvt. Ltd., India
Disodium EDTA	Himedia, India
Triethanolamine	Loba Chemie Pvt. Ltd., India

Table 5.2 List of Equipments

Equipment/Instrument	Manufacturer/Supplier
Digital Analytical Balance	Shimadzu, Japan
RP-HPLC with UV detector (gradient)	Agilent, Germany
pH meter	Lab India Pvt. Ltd., Mumbai
Magnetic Stirrer	Remi equipment Pvt. Ltd., India
Vortex mixer	Spinix, Japan
Ultraturrax T25	IKA, Mumbai
Probe Sonicator	Labman Scientific Instruments Pvt. Ltd.
Centrifuge	Remi Instrument, India
Bath Sonicator	Remi equipment Pvt. Ltd., India
Particle Size Analyser (Nano-ZS)	Malvern Instrument, UK
Distillation assembly	Durga glassware, India
Brookfield Viscometer	Brookfield Engineering Laboratories, USA
Transmission electron microscope	JEOL, Japan

5.3 Methodology

5.3.1 Preparation of Luliconazole loaded Nanoemulsion (LZNE) and Tavaborole loaded Nanoemulsion (TBNE):

The LZNE and TBNE were synthesized using a high-energy technique (13). A oil phase was made up of 21% w/w capmul MCM C8 and 9% w/w coconut oil as oil, 1% w/w Luliconazole or 5% w/w Tavaborole (API) and 2% cremophore EL as surfactant and stirred at 1000 RPM for 30 minutes. While aqueous phase was made up of 66% water and 1% pluronic F 127 and stirred at 1000 RPM for 30 minutes. The oil phase containing the drug was then incrementally introduced into the aqueous phase at 15,000 RPM using an ultra turrax to create a coarse emulsion. This emulsion was further refined into a fine nanoemulsion through probe sonication at 80 watts for two cycles of one minute each.

5.3.2 Implementing QbD for Formulation Development:

It is essential to identify the formulation, process, and environmental variables that could impact the characteristics of the final product before commencing any formulation process. The

variables associated with the production of a LZNE and TBNE via a high-energy method were delineated using an Ishikawa diagram (refer to Figure 5.1).

5.3.2.1 Quality Target Product Profile (QTPP):

In establishing a reliable, accurate, and repeatable production process, the following attributes were considered essential for the Quality Target Product Profile (QTPP).

- Globule size
- %EE
- % Drug release from nanoformulations

Globule size and %EE were selected as critical quality attributes (CQA) based on extensive literature review and preliminary experiment findings (14).

5.3.2.2 Formulation Optimization Using Box-Behnken Design (BBD):

Optimization through the method of varying one factor at a time offers a detailed examination of how each variable influences the outcome of an experiment, as opposed to altering all variables concurrently. The BBD methodology is a three-tiered design that integrates elements of incomplete block designs with two-level factorial designs. This cubic design is distinct from the 3-factor, 3-level Full Factorial Design and Central Composite Design (CCD) because it necessitates fewer experimental runs and includes mid-edge points along with a central replicate point. BBD's spherical design space provides excellent predictability within its bounds. Moreover, BBD is particularly effective for exploring quadratic response surfaces when the model does not require predictions at extreme levels (15). Table 5.3 outlines the chosen values for the BBD variables, encompassing both independent and dependent variables (response parameters).

Table 5.3 Selected values of variables for BBD

Variables	Levels (-1, 0, 1)
Independent variables	
A: %Oil Concentration	20,30,40
B: %Smix Concentration	2,3,4
C: Homogenization Speed	12000, 15000,18000
Dependent variables (response parameters)	
Globule size (Y1)	

%EE (Y2)

Key formulation factors were identified based on initial research findings. Utilizing Stat-Ease Design-Expert Software version 13.0, a BBD design matrix was generated, resulting in 17 experimental runs. All LZNEs and TBNEs were prepared following the design matrix, with other process variables kept constant. The globule size and %EE of the nanoemulsions were measured as response parameters (CQA).

5.3.2.3 Preparation of checkpoint batches as per the overlay plot

After deriving and adding the data of the prepared batches based on the BBD, the data was analyzed by employing Design Expert 13.0 for optimized area. Checkpoint batches were prepared according to the three randomized points which were selected from the optimized area.

5.3.3 Analysis of LZNE and TBNE:

5.3.3.1 Measurement of Globule Size, PDI, and Zeta Potential:

A sample of the nanoemulsion was diluted tenfold with pre-filtered distilled water and placed into a disposable sizing cuvette. The sample's globule size, polydispersity index (PDI), and zeta potential were then assessed using dynamic light scattering (DLS) with a Nano-ZS Zetasizer from Malvern Instruments Ltd., UK (16).

5.3.3.2 Determination of %EE:

The percentage of drug encapsulation was determined by centrifuging the nanoemulsion at 14,000 rpm for 20 minutes at 5°C. The precipitate formed represents the free drug while entrapped drug remained in supernant. The supernant was collected and dissolved in a methanol and analyzed using a validated analytical method (mentioned in 3.3.2 and 3.4). To ensure mass balance, the sedimented part was also examined for free Luliconazole and Tavaborole developed UV and HPLC method respectively (17).

$$\%Entrapment\ efficiency\ (\%EE) = \left(\frac{amount\ of\ entrapped\ drug}{total\ drug\ added}\right) x\ 100$$

5.3.3.3 Evaluating the Thermodynamic Stability of LZNE and TBNE:

To ensure the long-term stability of formulations, physical thermodynamic stability assessments were conducted.

5.3.3.3.1 Centrifugation Analysis:

The physical stability of nanoemulsion was assessed by observing the effects of centrifugation on its characteristics. The formulation underwent centrifugation at speeds ranging from 4000 to 10,000 rpm, each for 20 minutes, and was then examined for any signs of phase separation (18).

5.3.3.3.2 Heating-Cooling Cycles:

The impact of temperature fluctuations on nanoemulsion stability was monitored through six cycles alternating between 4°C and 40°C, with each temperature maintained for at least 48 hours. The formulations underwent a heating cooling cycle test to verify their stability under these conditions (19).

5.3.3.3.3 Freeze-Thaw Cycles:

Formulations were subjected to three freeze-thaw cycles ranging from -21°C to +25°C, with each temperature phase lasting no less than 48 hours. Only those formulations that successfully endured these thermodynamic stability tests were selected for further study (20).

5.3.3.4 % Transmittance Measurement

The clarity of the developed formulations was quantified using a UV spectrophotometer, measuring the % transmittance at 630 nm in triplicate for samples of 5 ml (21).

5.3.3.5 Assay

Quantification of Luliconazole and Tavaborole in LZNE and TBNE was conducted using an UV spectrophotometric method and HPLC method respectively. The drug content was quantified as the percentage of Luliconazole and Tavaborole detected in the formulation relative to the initial drug quantity added. For the drug content determination, 1.0 ml of LZNE (containing approximate 10 mg Luliconazole) was appropriately diluted with methanol and then analyzed via UV visible Spectrophotometry for Luliconazole (22). Similarly 1.0 ml of TBNE (containing approximate 50 mg Tavaborole) was appropriately diluted with methanol and then analyzed by HPLC for Tavaborole (23).

5.3.3.6 Differential Scanning Calorimetry (DSC)

Thermal analysis of the drug was performed using a DSC-41 (Shimadzu, Japan). A sample weighing 2-3 mg was enclosed in an aluminum pan under pressure and heated from 25°C to 300°C at a rate of 10°C/min. A nitrogen flow of 40 ml/min was maintained to provide an inert atmosphere and prevent oxidation (24).

5.3.3.7 Transmission Electron Microscopy (TEM)

The droplets of LZNE and TBNE were examined using negative-staining electron microscopy to assess their size and morphology. Samples were placed on carbon-coated copper/palladium grids for one minute, rinsed thrice with sterilized, deionized water, and then negatively stained with 2% (w/v) ammonium molybdate at pH 6.5 for one minute before TEM analysis using a JEOL JEM 2100 microscope at 100 kV (25).

5.3.3.8 Powder X-Ray Diffraction Studies

X-ray diffraction analysis was employed to investigate the crystalline structure of Luliconazole and the lyophilized LZNE (Lyophilization parameters: freezing stage -40 ºC, drying at 20 ºC, vaccum 120 mm Hg, time 48 hrs). Using a Rigaku-Miniflex diffractometer with a Cu anode and K radiation, the solid samples were scanned over a 2θ range of 10–40º at an accelerating voltage of 30 kV and temperature of 25ºC (26).

5.3.4 Gel Formulation of LZNE and TBNE

Optimized LZNE and TBNE were converted to gel formulation to enhance the viscosity of developed formulations for improved adherence to the skin. Carbopol 974P was chosen as the gelling agent for its superior hydrating and wetting characteristics (27). Initially, Carbopol 974P (1% w/v) was uniformly dispersed in the Luliconazole nanoemulsion (1% w/v) using magnetic stirrer at 2000 rpm for an hour. To this mixture, 4% w/w Propylene glycol was added while stirring continuously. The gel's pH was adjusted to between 5.5 and 6.5 using triethanolamine to convert mixture into gel formation.

5.3.5 Characterization of the Optimized Nanoemulsion Gels

5.3.5.1 Gel Viscosity

The viscosity of the gel was measured with a Brookfield DV-I prime model viscometer, employing a T-bar No. 96 spindle (28).

5.3.5.2 pH Measurement of Gel

The pH level of the formulated gels was determined using a standard pH meter (Lab India Pvt. Ltd., Mumbai) (29).

5.3.5.3 Gel Spreadability

The spreadability of free Luliconazole gel, LZNE containing gel, free Tavaborole gel and TBNE containing gel was assessed by a following method. A fixed quantity (150 mg) of each gel was placed within a marked circle on a glass plate, covered with another glass plate, and subjected to

a weight of 10 g for five minutes; the time that needed for upper plate to completely separate from the lower plate is measured. Spreadability was determined by the below equation (30).

$$Spreadability = \frac{M\ x\ L}{T}$$

Where, M – weight in gm placed on upper plate, L – length of plate, T – time taken to separate

5.3.5.4 Assay of gel

The content of Luliconazole and Tavaborole in all gel formulations was quantified by dissolving 100 mg of each sample in methanol and analyzing them using a UV Spectrophotometry and HPLC method respectively (31).

5.3.5.5 Gel Strength Testing

The mechanical properties of the nanoemulsion-based gel were evaluated using a texture analyzer (CT3, Brookfield Engineering) with a 10 kg load cell. The gel was placed into a cone fixture and allowed to settle at room temperature for 15 minutes before testing with a probe (TA3/100) under specified conditions (Pre-test speed of 1 mm/s and test speed of 0.5 mm/s) to assess its strength (32).

5.4 Results and Discussion

5.4.1 Formulation Development of LZNE and TBNE

5.4.1.1 Defining QTPP

Table: 5.4 QTPP and CQA elements with justification for LZNE

QTPP elements		Target	Justification
Route of administration		Topical	To effective permeation of drug and deposition of drug in skin for better topical delivery of product and reduce systemic side effect.
Dosage form		Nanoemulsion	Better skin permeability, controlled release of drug
Formulation quality attributes	Globule size*	Optimum	For better permeation as well as skin deposition. To prevent drug entry in blood circulation.
	Polydispersity index (PDI)	Minimum (<0.3)	To ensure formation of monodisperse formulation
	Shape	Globules	To ensure formation of nanoemulsion
	Zeta potential	>±30 mV	For the enhancement of stability of the dispersion
	%EE *	Maximize	For the reduction of cost, drug wastage to be Reduced
	In-vitro drug release	For 24 hrs	To ensure controlled release of drug.
Ex-vivo permeability		Maximize	To ensure effective permeation of drug.
Stability		Not less than 3 month	For ensuring stability of developed formulation during its complete shelf life
Safety		Non-toxic and non-irritant to skin	To ensure prevent skin irritation and cell toxicity
Pharmacodynamic		Similar or better than marketed product	For the illustration of therapeutic efficacy

* Critical Quality Attributes (CQAs)

5.4.1.2 Identification of independent variables and qualitative risk assessment using Ishikawa diagram

The factors influencing the creation of LZNE and TBNE by high-energy method were categorized into three groups: formulation, process, and environmental variables. An Ishikawa diagram (refer to figure 5.1) was utilized to illustrate these contributing factors.

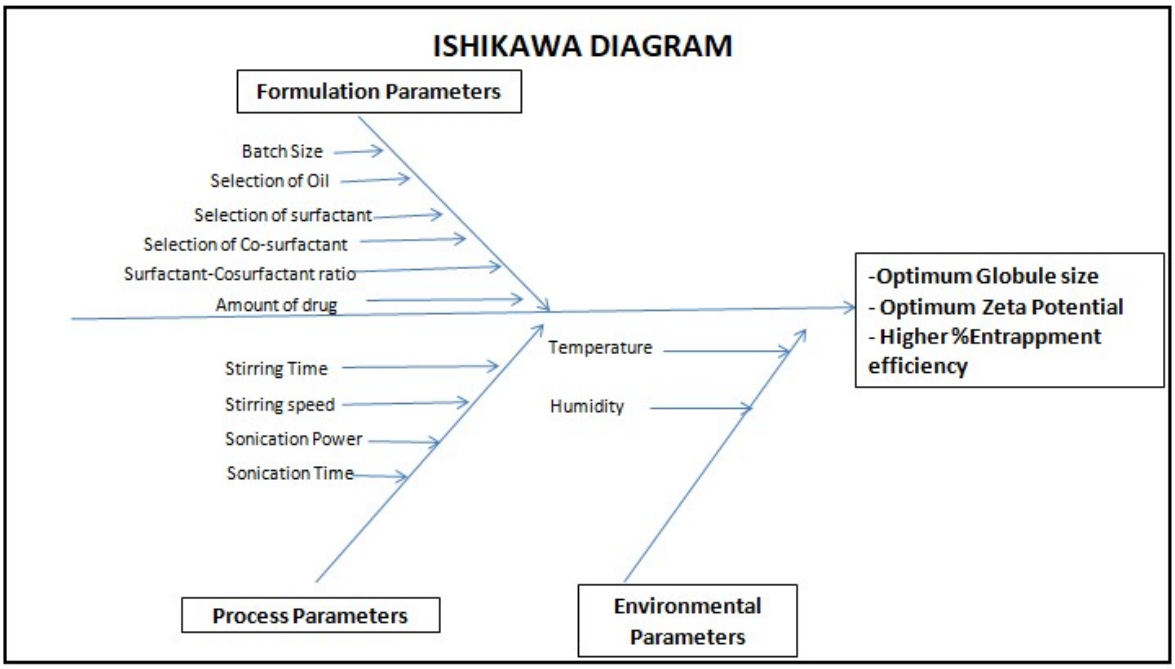

Figure 5.1 Ishikawa diagram showing probable variables that may influence CQA

5.4.2 Formulation optimization by Box-Behnken Design for Luliconazole loaded Nanoemulsion

Based on the preliminary investigation, three critical parameters were identified, and their relationship with critical quality attributes (CQA) was exhaustively investigated using Box-Behnken Design. A randomized matrix of 17 runs was generated by Design-Expert software and presented in table 5.5.

Table 5.5: Randomized BBD design matrix generated Design-Expert software

Run	Independent Variables			Dependent Variables (CQA)	
	A: Oil Concentration (%)	B: Smix Concentration (%)	C: Homogenization Speed (RPM)	Globule size (nm)	%EE
1	30	2	18000	192.54±0.21	71.94±0.55
2	40	4	15000	201.09±1.06	78.49±1.08
3	40	2	15000	246.61±0.58	73.61±1.38
4	40	3	12000	237.91±0.22	78.32±0.64
5	30	2	12000	246.01±1.54	69.31±1.28
6	30	4	12000	189.64±1.39	77.93±0.57
7	20	2	15000	196.37±0.93	52.71±0.68
8	30	3	15000	232.09±1.73	80.33±1.72
9	30	3	15000	233.15±0.05	80.75±0.53
10	40	3	18000	202.37±1.64	77.31±1.67
11	30	3	15000	243.97±0.84	79.93±0.82
12	20	4	15000	193.06±1.44	67.43±0.77
13	30	3	15000	242.89±1.73	81.19±0.93
14	30	4	18000	203.22±0.97	79.11±1.09
15	20	3	18000	202.09±1.94	59.16±1.64
16	20	3	12000	195.33±0.61	54.21±0.27
17	30	3	15000	231.95±0.49	78.32±1.19

From the table 5.5 it can be concluded that as the oil concentration decreases %EE decreases. It may be because of Luliconazole is lipophilic drug and entrapped in the oil phase. Luliconazole has a partition coefficient (log P) of 4.07 (33) which indicate higher affinity towards oil phase. It may be possible reason for the enhancement of %EE with the increment in oil phase concentration.

5.4.2.1 Effect analysis of critical variables on responses

5.4.2.1.1 Influence of investigated parameters on globule size

A) Statistical Analysis for Globule size

The statistical analysis of the design mentioned above is as follows:

Table 5.6 Statistical analysis of design for Globule size

Source	Sequential p-value	Lack of Fit p-value	Adjusted R^2	Predicted R^2	
Linear	0.1042	0.0116	0.2209	-0.0677	
2FI	0.1424	0.0160	0.3979	0.1362	
Quadratic	**0.0002**	**0.7757**	**0.9409**	**0.8775**	**Suggested**
Cubic	0.7757		0.9194		**Aliased**

As shown in table 5.6, the best model to fit the experimental results of globule size in nanoemulsion is the quadratic model and was chosen for further evaluation.

B**) ANOVA Analysis for Globule size**

The ANOVA for globule size is given in below table 5.7.

Table 5.7 ANOVA for Response Surface Quadratic Model for globule size

Source	Sum of Squares	Df	Mean Square	F- value	p-value	
Model	7856.90	9	872.99	29.32	< 0.0001	Significant
A-Oil Concentration	1261.78	1	1261.78	42.38	0.0003	
B-Smix Concentration	1109.68	1	1109.68	37.27	0.0005	
C-Homogenization Speed	588.42	1	588.42	19.76	0.0030	

AB	443.52	1	443.52	14.90	0.0062	
AC	470.67	1	470.67	15.81	0.0054	
BC	1156.00	1	1156.00	38.83	0.0004	
A^2	708.76	1	708.76	23.81	0.0018	
B^2	924.99	1	924.99	31.07	0.0008	
C^2	896.81	1	896.81	30.12	0.0009	
Residual	208.40	7	29.77			
Lack of Fit	45.90	3	15.30	0.3767	0.7757	not significant
Pure Error	162.49	4	40.62			
Cor Total	8065.30	16				

The Model's F-value of 29.32 suggests that the model is significant. The likelihood of such a high F-value occurring by chance is only 0.01%.

P-values below 0.0500 signify that the model terms are significant. For this particular model, the terms A, B, C, AB, AC, BC, A^2, B^2, and C^2 are considered significant. Conversely, values above 0.1000 suggest that the model terms are not significant. Reducing the number of insignificant model terms (excluding those necessary for hierarchy) could potentially enhance the model.

An F-value of 0.38 for Lack of Fit indicates that it is not significant when compared to pure error. There's a 77.57% probability that such a Lack of Fit F-value could arise by random variation. A non-significant Lack of Fit is desirable as it indicates a good fit for the model.

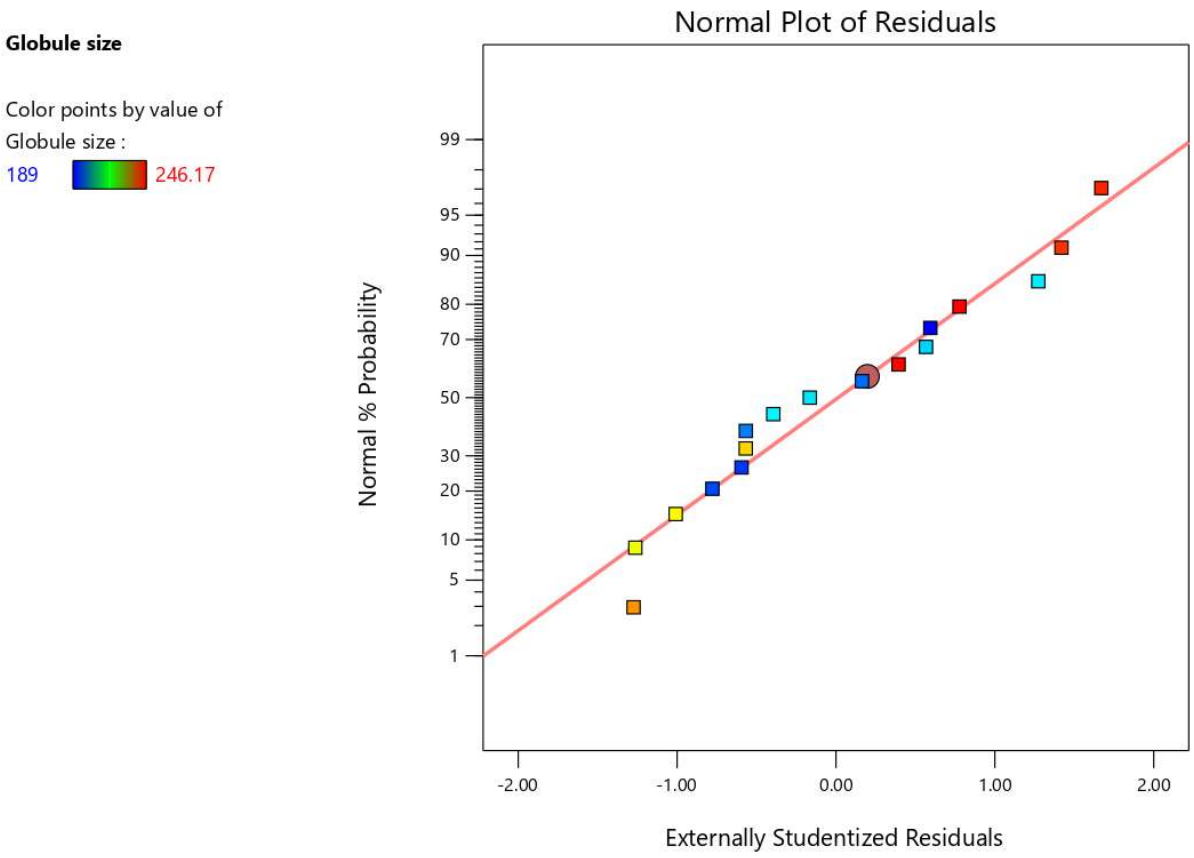

Figure 5.2 Actual v/s Predicted plot for % globule size

Table 5.8 ANOVA study results for globule size

Parameters	Results of Response
Std Deviation	5.46
Mean	216.97
C.V.%	2.51
R-Squared	0.9742
Adjusted R-Squared	0.9409
Predicted R-Squared	0.8775
Adeq. Precision	13.7535

The Predicted R^2 value of 0.8775 aligns well with the Adjusted R^2 value of 0.9409, indicating a discrepancy of less than 0.2. The Adequate Precision metric, which assesses the signal-to-noise

ratio, shows a value of 13.753, suggesting a robust signal since a value above 4 is preferable. This suggests that the model is reliable for navigating within the design space.

C) Regarding the Mathematical Model for Globule Size

The influence of different factors on globule size was analyzed using contour and 3D plots, supported by ANOVA data presented in Table 5.8. It is evident that varying levels of factors alter the globule size, confirming their impact. A detailed examination of each factor reveals the magnitude and direction (positive or negative) of their effects on globule size.

The final equation in terms of coded factors:

Globule size: $+236.92+12.56*A-11.78*B-8.58*C-10.53*AB-10.85*AC+17.00*BC-12.97*A^2-14.82*B^2-14.59*C^2$

Table 5.9: The Final equation in terms of actual factors

Globule Size	=
+236.92	
+12.56	Oil Concentration
-11.78	S_{mix} Concentration
-8.58	Homogenization speed
-10.53	Oil Concentration * S_{mix} Concentration
-10.85	Oil Concentration * Homogenization speed
+17.00	S_{mix} Concentration * Homogenization speed
-12.97	Oil Concentration^2
-14.82	S_{mix} Concentration^2
-14.59	Homogenization speed^2

The presence of a positive sign preceding a factor signifies an increase in response with the factor and vice versa. One of the three independent variables that were selected has positive effects on globule size and two of the three independent variables that were selected have

negative effects on globule size as shown by the coefficient values of the individual factors. However, combinations of factors like 1. oil concentration and S_{mix} concentration 2. oil concentration and homogenization speed show negative effect while combination of S_{mix} concentration and homogenization speed shows positive effect on globule size. Moreover, the equation above shows that every component affects globule size to some extent. The highest co-efficient value before factor A indicates that oil concentration has the greatest impact on globule size, which is followed by S_{mix} Concentration and homogenization speed. The equation also reveals that each factor contributes to the variation in globule size. Notably, a higher concentration of oil correlates with an enlargement of globule size. Equation also showed that with increase in surfactant concentration, there is a decrease in globule size. A higher concentration of surfactant lowers surface tension and aids in globule stabilization. The globule size is negatively impacted by homogenization speed, as the equation illustrates; that is, as homogenization speed increases, globule size decreases. It may be because of the disruption of the globules caused by an increase speed of homogenization (34).

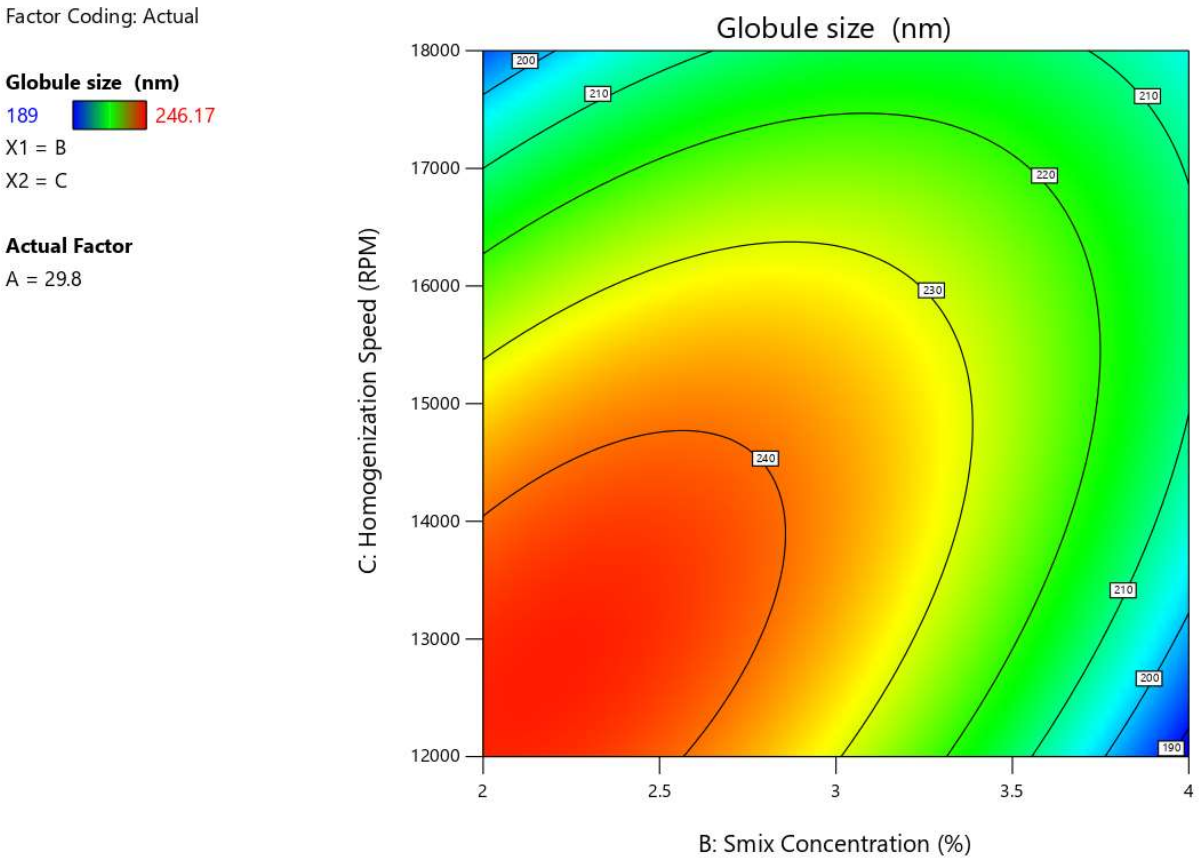

Figure 5.3 Contour plot (2D) showing the combined effect of Smix concentration and homogenization speed on globule size

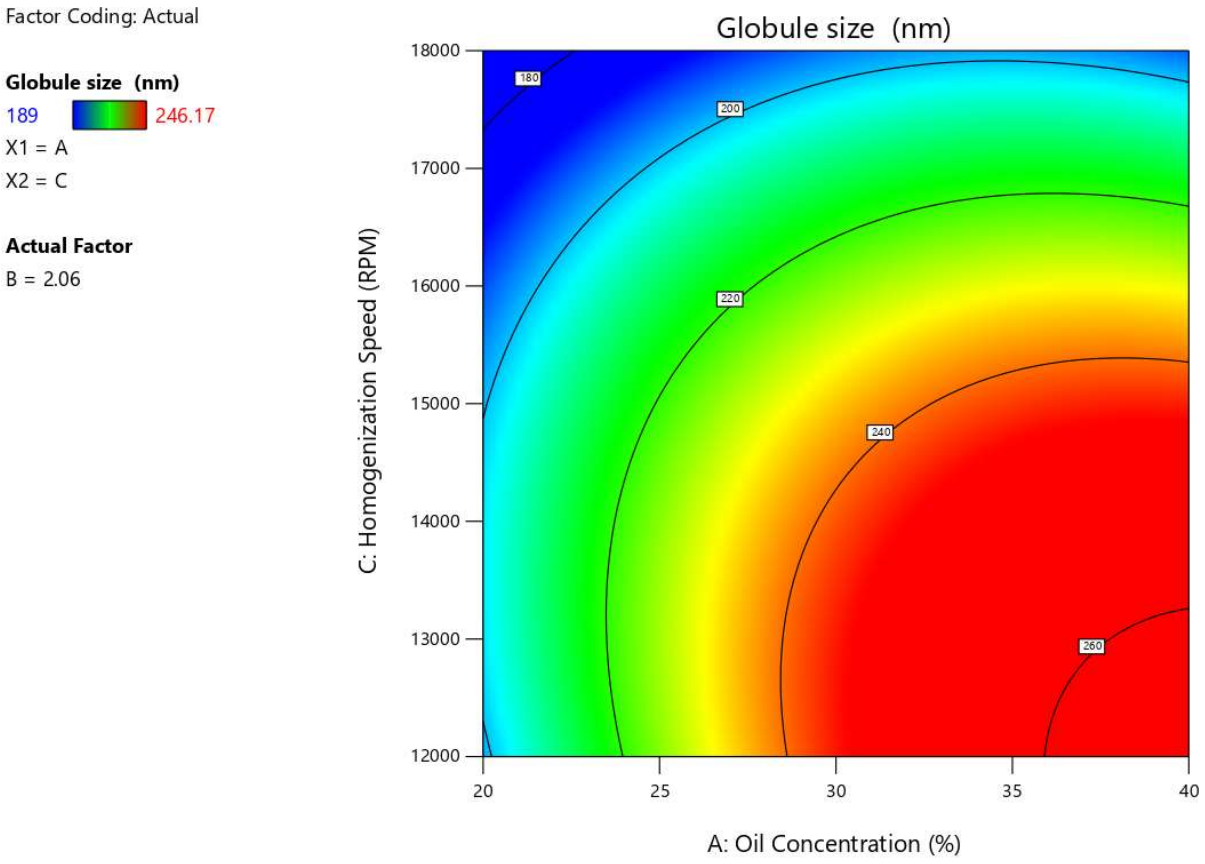

Figure 5.4 Contour plot (2D) showing the combined effect of oil concentration and homogenization speed on globule size

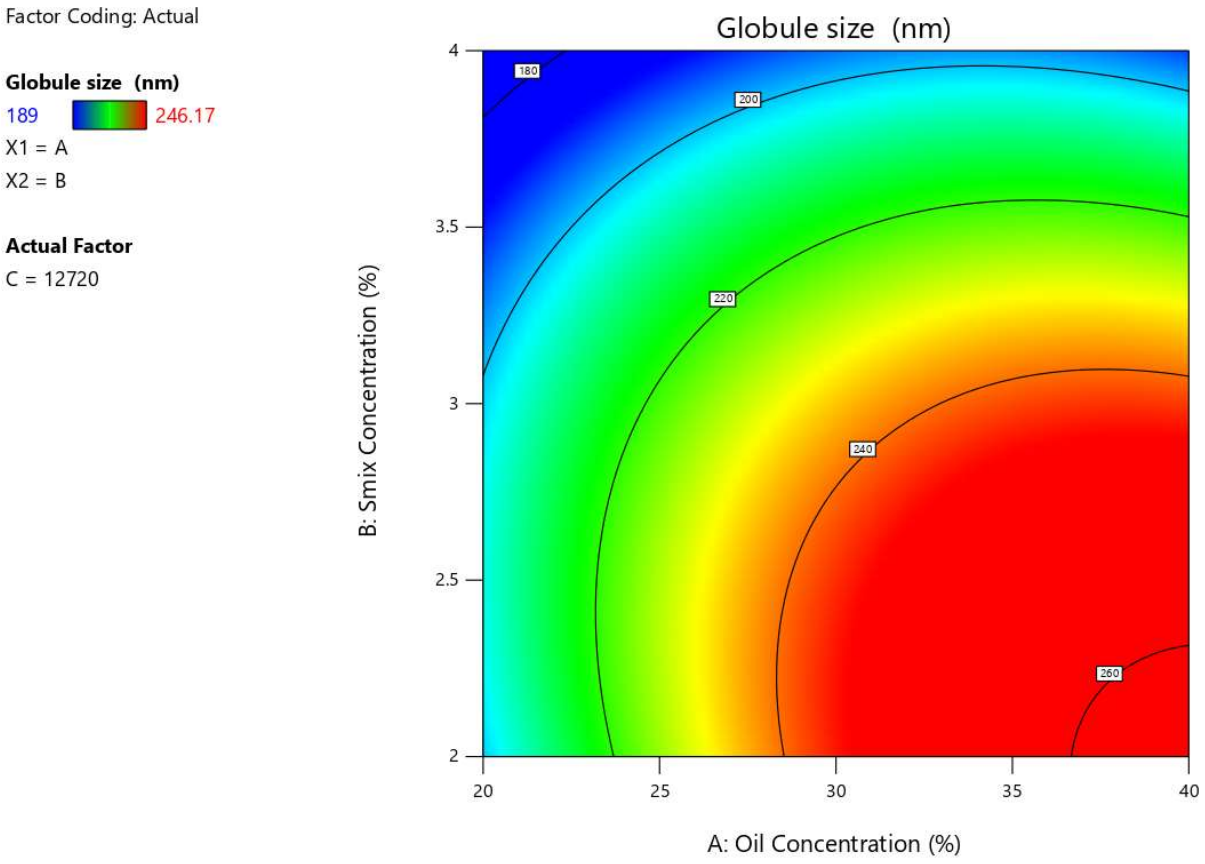

Figure 5.5 Contour plot (2D) showing the combined effect of oil concentration and Smix concentration on globule size

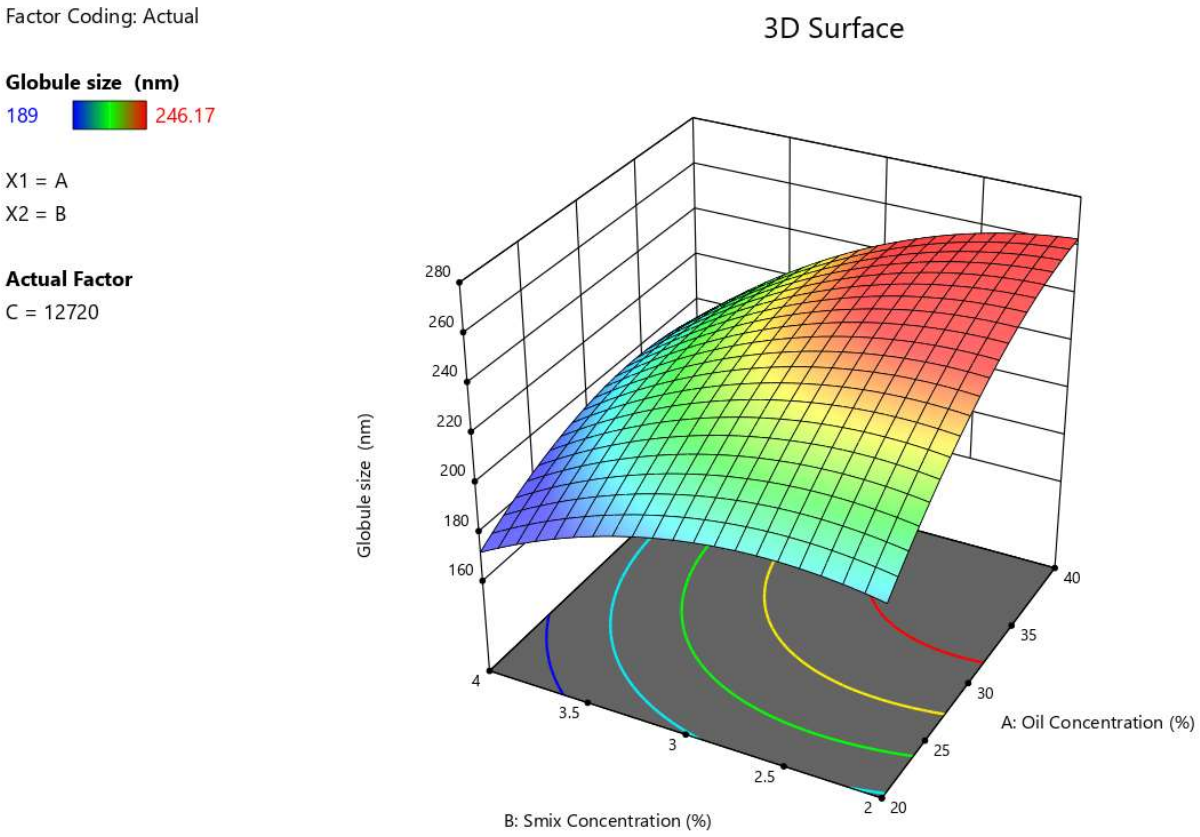

Figure 5.6 Response surface (3D) showing the combined effect of Smix concentration and Oil concentration on globule size

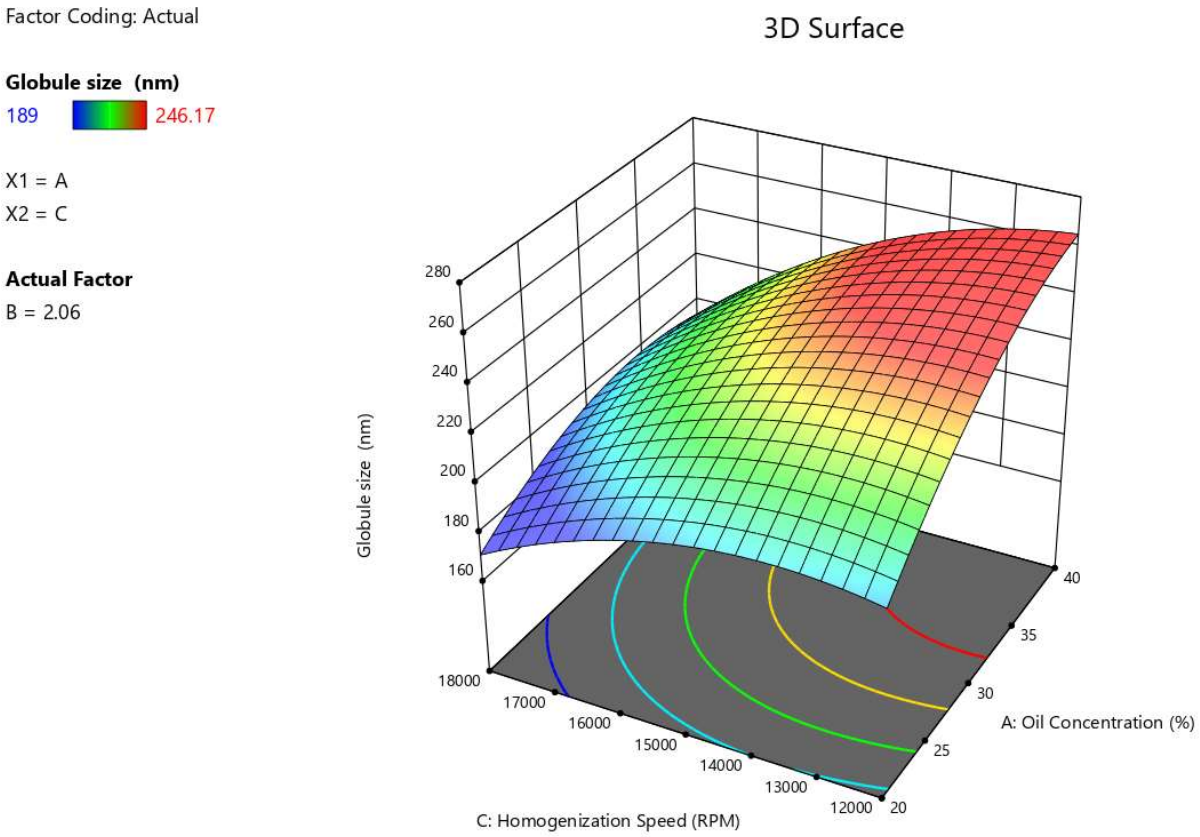

Figure 5.7 3D surface graph showing the combined effect of oil concentration and homogenization speed on globule size

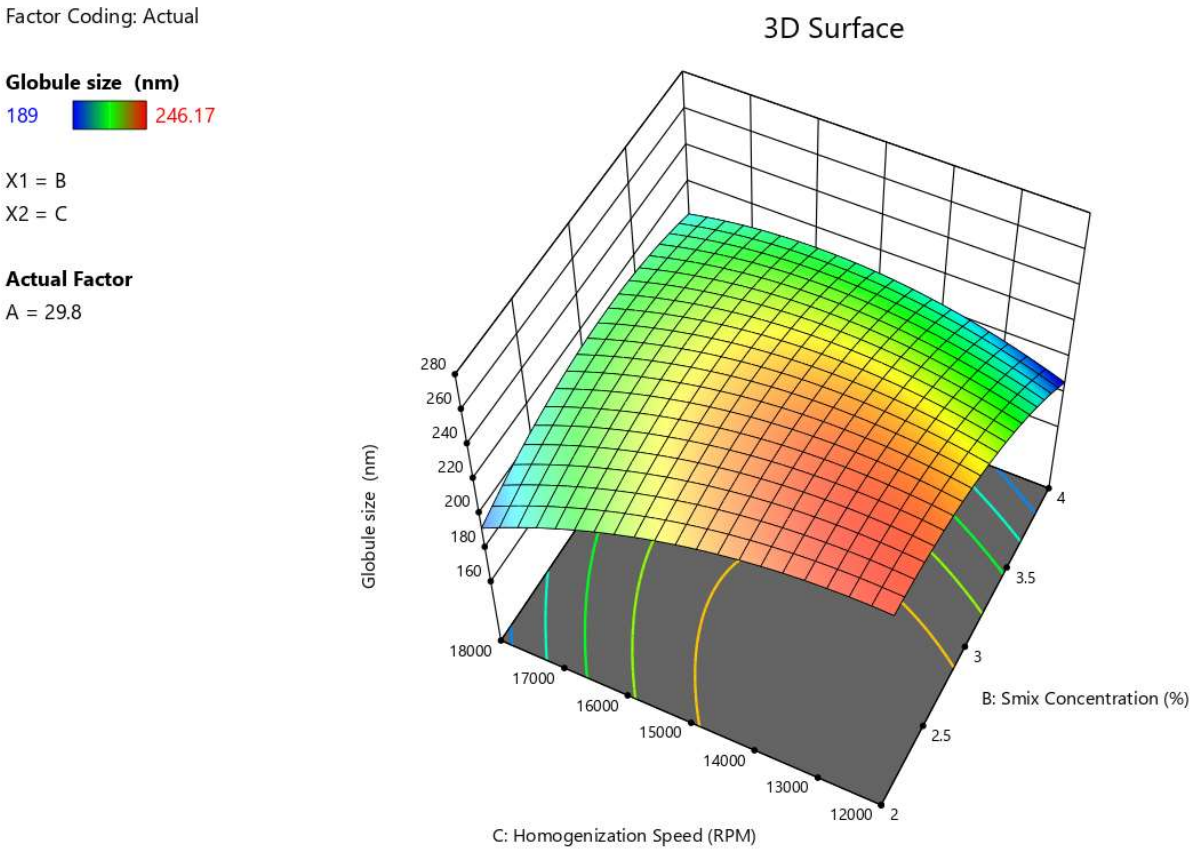

Figure 5.8 3D surface graph showing the combined effect of S_{mix} concentration and homogenization speed on globule size

The effects of independent factors on the globule size are shown in Fig. 5.3 to figure 5.8. The highest globule size is shown by the red area, and the lowest globule size is represented by the blue zone. It can be observed that as the oil concentration increases the globule size increases. It can be observed depicted that as the S_{mix} concentration and homogenization speed increases the globule size decreases (34). These graphs show the relationship between the CQA and the corresponding independent factor while maintaining constant levels of the other independent variables.

5.4.2.1.2 Influence of investigated parameters on %EE

A) Statistical Analysis for %EE

The statistical analysis of the design mentioned above is as follows:

Table 5.10 Statistical analysis of design for %EE

Source	Sequential p-value	Lack of Fit p-value	Adjusted R^2	Predicted R^2	
Linear	0.0054	0.0010	0.5198	0.3633	
2FI	0.8811	0.0005	0.4141	-0.1324	
Quadratic	**< 0.0001**	**0.1019**	**0.9674**	**0.8220**	**Suggested**
Cubic	0.1019		0.9861		**Aliased**

As shown in table 5.10, the best model to fit the experimental results of %EE in nanoemulsion is the quadratic model and was chosen for further evaluation.

B**) ANOVA Analysis for %EE**

The ANOVA for globule size is given in below table.

Table 5.11 ANOVA for Response Surface Quadratic Model for %EE

Source	Sum of Squares	Df	Mean Square	F- value	p-value	
Model	1378.29	9	153.14	53.77	< 0.0001	Significant
A-Oil Concentration	688.58	1	688.58	241.74	< 0.0001	
B-Smix Concentration	156.56	1	156.56	54.96	0.0001	
C-Homogenization Speed	7.51	1	7.51	2.64	0.1485	
AB	24.21	1	24.21	8.50	0.0225	
AC	8.88	1	8.88	3.12	0.1208	
BC	0.5256	1	0.5256	0.1845	0.6804	
A^2	394.80	1	394.80	138.61	< 0.0001	
B^2	23.47	1	23.47	8.24	0.0240	
C^2	42.33	1	42.33	14.86	0.0063	

Residual	19.94	7	2.85			
Lack of Fit	15.08	3	5.03	4.14	0.1019	not significant
Pure Error	4.86	4	1.22			
Cor Total	1398.23	16				

The significant Model F-value of 53.77 suggests that the model is reliable. The likelihood of achieving such a high F-value by chance, due to noise, is as low as 0.01%.

Model terms with P-values below 0.0500 are considered significant. In this analysis, the terms A, B, AB, A^2, B^2, and C^2 are noteworthy. Conversely, terms with P-values above 0.1000 are deemed insignificant. Reducing the number of insignificant terms (excluding those necessary for hierarchical structure) might enhance the model.

An insignificant Lack of Fit F-value of 4.14, relative to pure error, indicates a good model fit, with a 10.19% probability that such a value could arise from noise alone. A non-significant lack of fit is desirable as it indicates the model's adequacy.

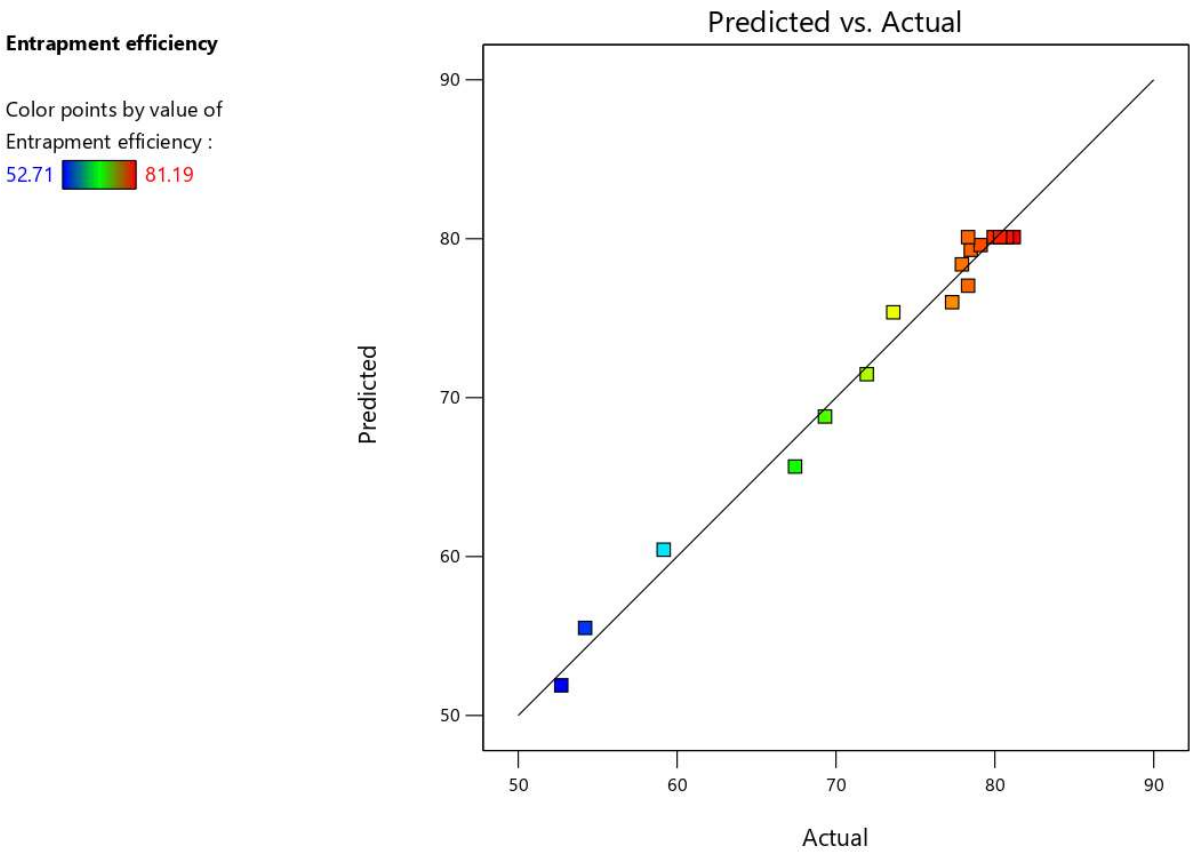

Figure 5.9 Actual v/s Predicted plot for %EE

Table 5.12 ANOVA study results for %EE

Parameters	Results of Response
Std Deviation	1.69
Mean	72.94
C.V.%	2.31
R-Squared	0.9857
Adjusted R-Squared	0.9674
Predicted R-Squared	0.8220
Adeq. Precision	21.7899

The **Predicted R²** of 0.8220 is in reasonable agreement with the **Adjusted R²** of 0.9674; i.e. the difference is less than 0.2.

Adeq Precision measures the signal to noise ratio. A ratio greater than 4 is desirable. Your ratio of 21.790 indicates an adequate signal. This model can be used to navigate the design space.

C) Mathematical Model for %EE

The impact of different factors on the percentage of %EE was analyzed by referencing contour and 3D plots, in conjunction with ANOVA values. Table 5.11 reveals that alterations in the factor levels lead to changes in the outcome, namely the percentage of %EE, thus verifying the influence of these factors. A detailed analysis of each factor helps to quantify their specific impact. The mathematical equation delineates whether these effects are positive or negative.

The final equation in terms of coded factors:

%EE: +80.10+9.28*A+4.42*B+0.9687*C-2.46*AB-1.49*AC-0.3625*BC-9.68*A^2-2.36*B^2-3.17*C^2

Table 5.13 The Final equation in terms of actual factors:

%EE	**=**
+80.10	
+9.28	Oil Concentration
+4.42	S_{mix} Concentration
+0.9687	Homogenization speed
-2.46	Oil Concentration * S_{mix} Concentration
-1.49	Oil Concentration * Homogenization speed
-0.3625	S_{mix} Concentration * Homogenization speed
-9.68	Oil $Concentration^2$
-2.36	S_{mix} $Concentration^2$
-3.17	Homogenization $speed^2$

The presence of a positive sign preceding a factor signifies an increase in response with the factor and vice versa. Each of the three independent variables that were selected has positive effects on drug entrapment, as shown by the coefficient values of the individual factors.

However, combinations of factors like 1. oil concentration and S_{mix} concentration 2. oil concentration and homogenization speed and 3. S_{mix} concentration and homogenization speed shows negative effect on drug entrapment. Moreover, the equation above shows that every component affects %EE to some extent. The highest co-efficient value before factor A indicates that oil concentration has the greatest impact on %EE, which is followed by S_{mix} Concentration and homogenization speed. As an example, %EE increases when oil concentration increases. Luliconazole partitioned into the oil phase, resulting in an increase in %EE with an increase in oil concentration. An increase in homogenization speed was shown to cause an increase in %EE. The larger oil globules may break up into numerous fine oil droplets as the stirring speed is increased, trapping as much of the drug as possible in the formulation's oil phase. Increase in Smix concentration also enhances the %EE. This increase could be the result of the drug becoming more soluble in the lipid when the surfactant concentration rises (35).

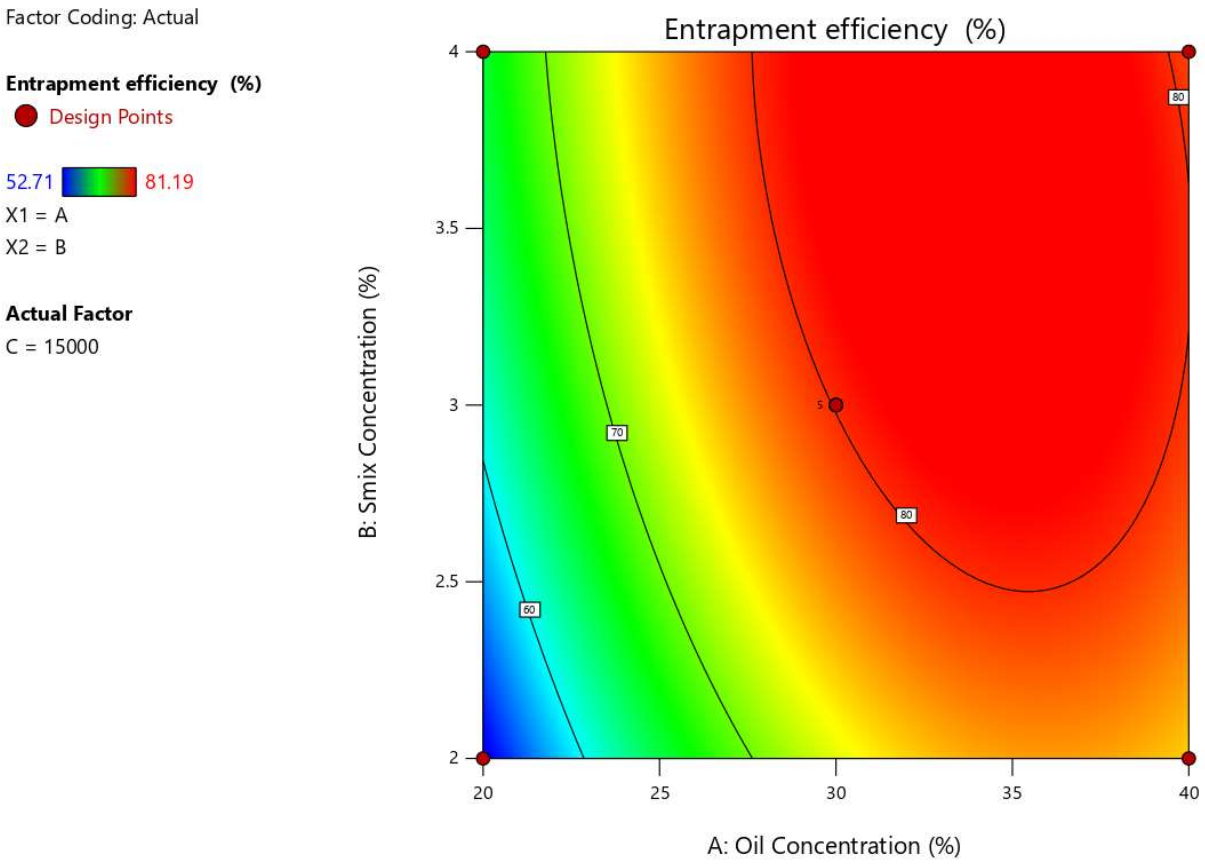

Figure 5.10 Contour plot (2D) showing the combined effect of Oil concentration and Smix Concentration on %EE

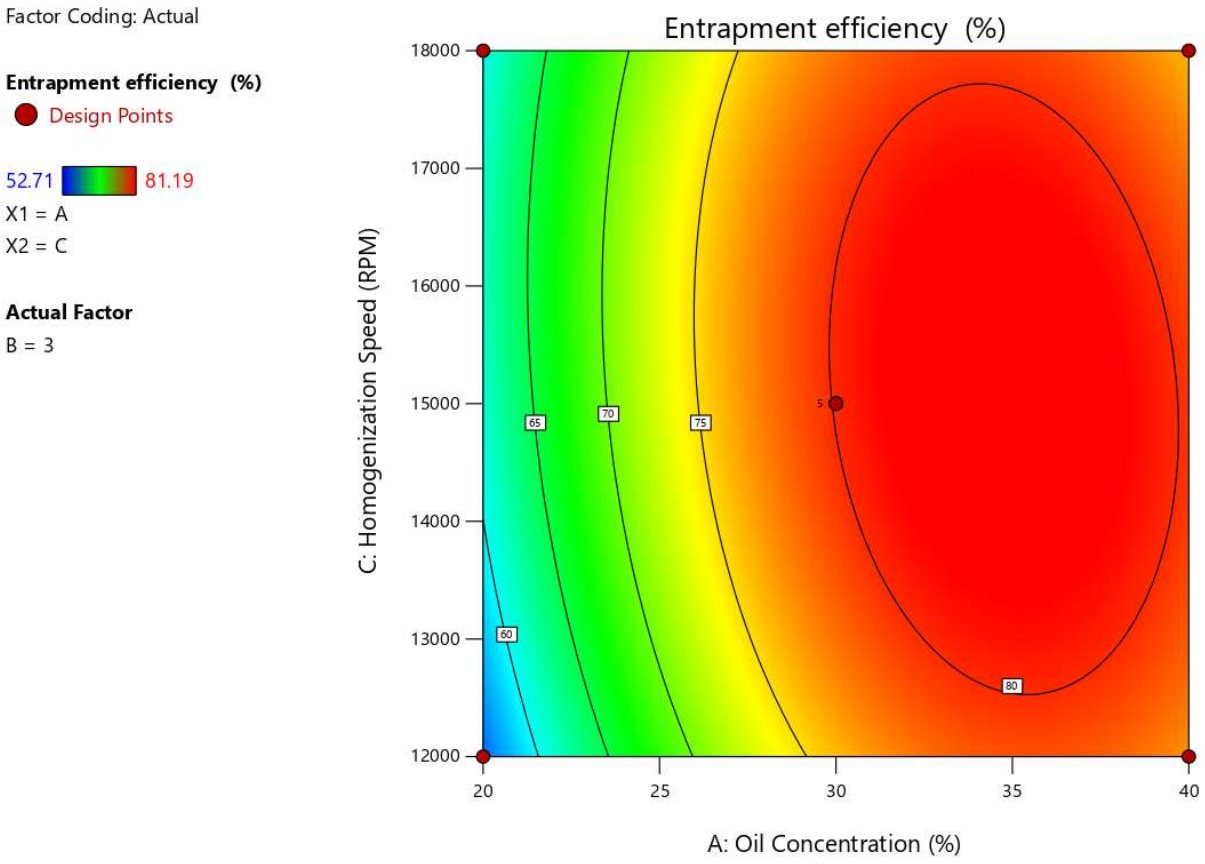

Figure 5.11 Contour plot (2D) showing the combined effect of Oil concentration and Homogenization speed on %EE

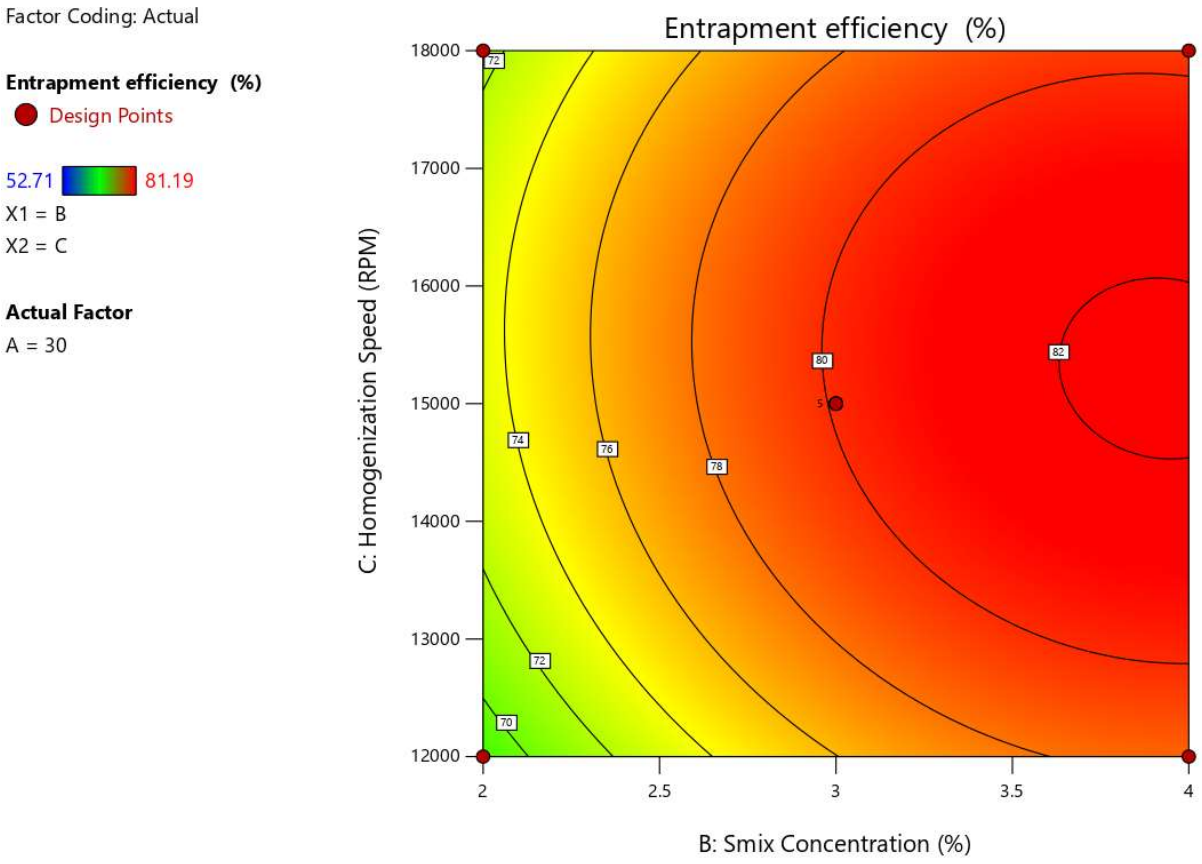

Figure 5.12 Contour plot (2D) showing the combined effect of Smix concentration and Homogenization speed on %EE

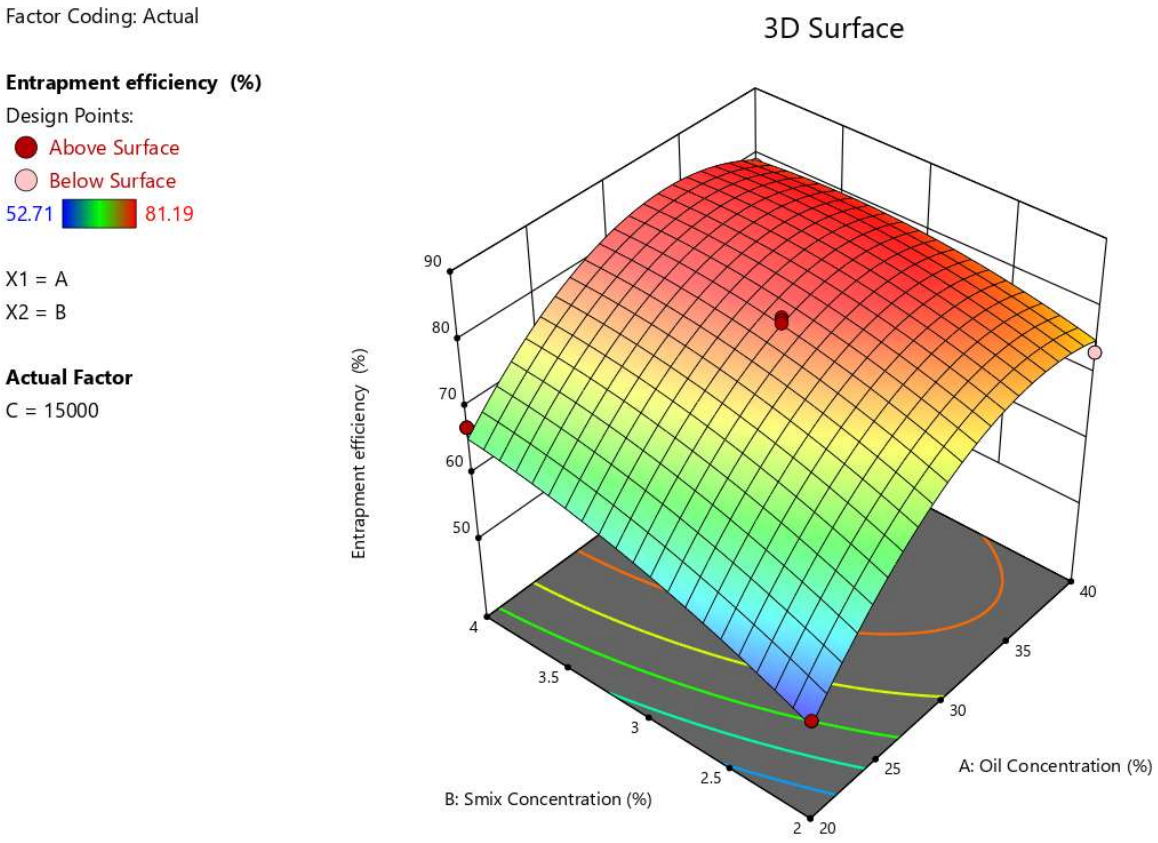

Figure 5.13 Response surface (3D) showing the combined effect of oil concentration and S_{mix} concentration on %EE

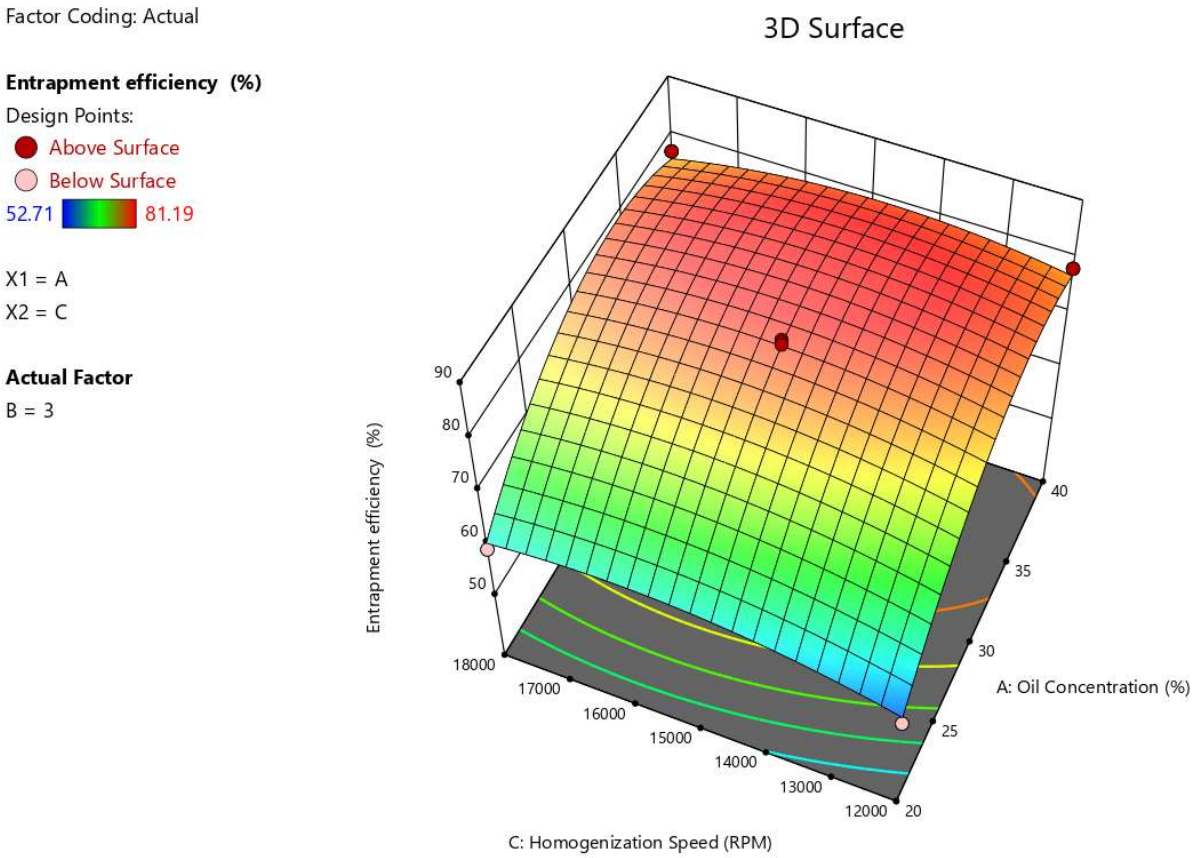

Figure 5.14 Response surface (3D) showing the combined effect of oil concentration and Homogenization speed on %EE

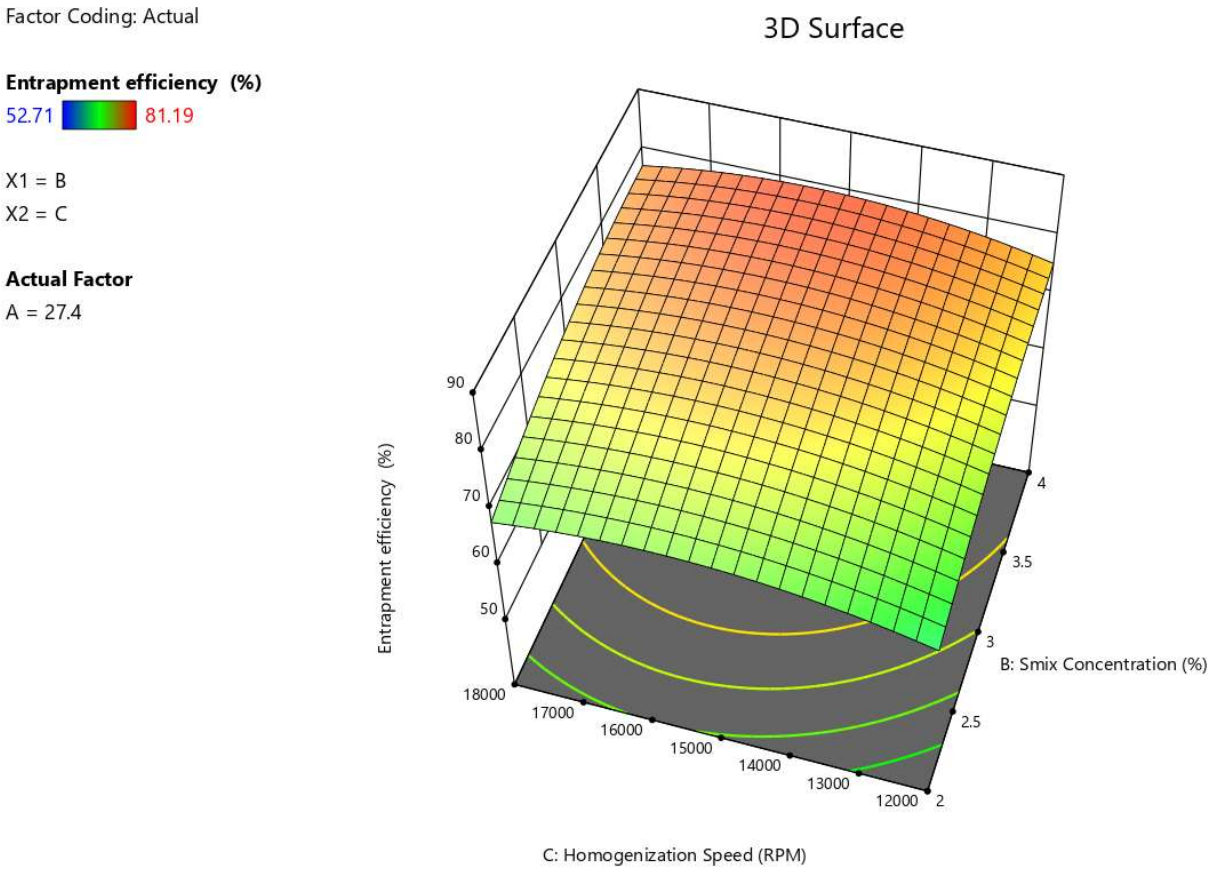

Figure 5.15 Response surface (3D) showing the combined effect of S_{mix} concentration and Homogenization speed on %EE

The effects of independent factors on the %EE are shown in figure 5.10 to figure 5.15. The highest %EE is shown by the red area, and the lowest %EE is represented by the blue zone. These graphs show the relationship between the CQA and the corresponding independent factor while maintaining constant levels of the other independent variables. It can be concluded that as the homogenization speed and oil concentration increases %EE increases. It is depicted that the drug entrapment increases with increase in the surfactant concentration. The reason for this increase may be an increase in solubility of the drug in the oil on increasing the concentration of the surfactant (35).

5.4.2.2 Preparation of checkpoint batches as per the overlay plot

Overlay contour plots for all two CQAs (%EE and globule size) were generated (Fig. 5.16) for obtaining the design space (yellow area in graph).

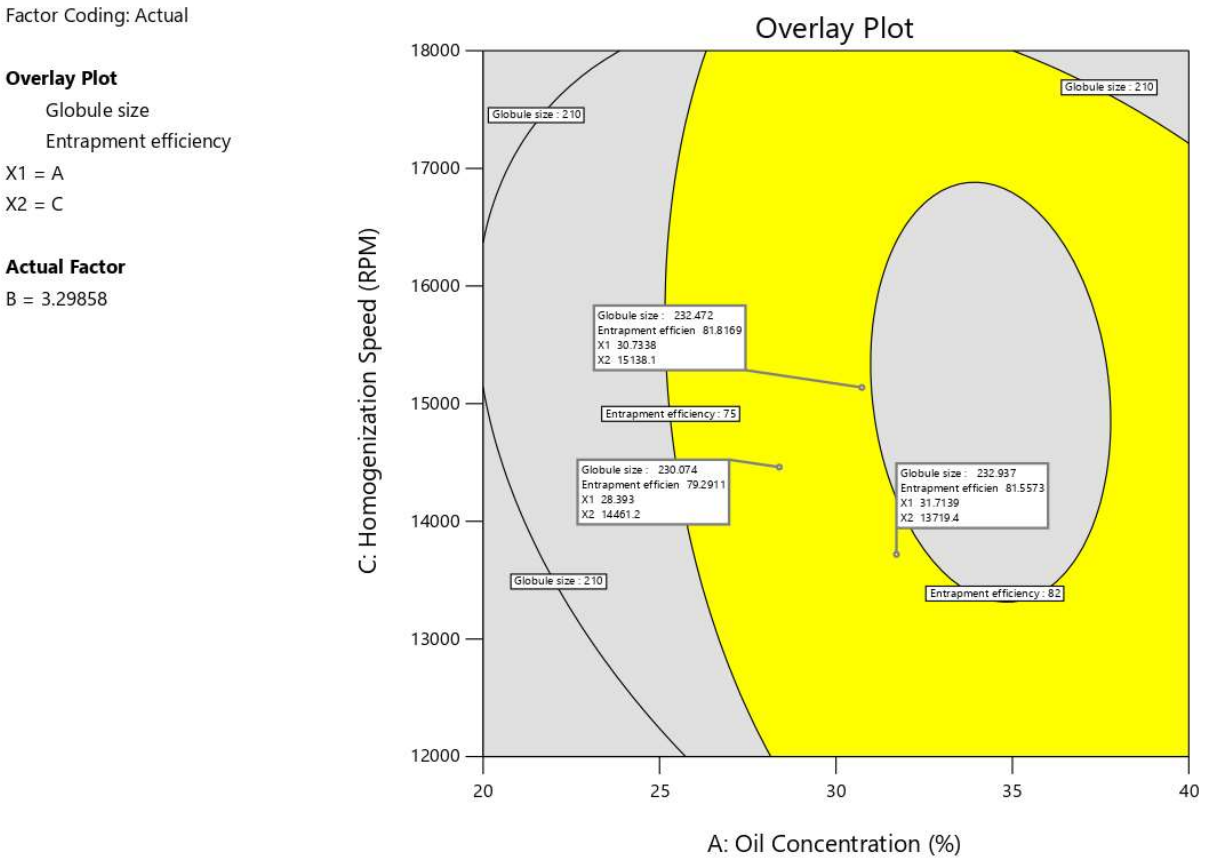

Figure 5.16 Overlay plot of LZ NE

Table 5.14: Results of check point batch and optimized batch for globule size and %EE

Batch	X1 (%Oil Concentration)	X2 (%S_{mix} Concentration)	X3 Homogenization speed)	Y1 (Globule Size)	Y2 (%EE)	Predicated Y1 (Globule Size)	Predicated Y2 (%EE)
Check point 1	30.73	3.29	15138.1	232.84	81.74	232.47	81.82
Check point 2	28.39	3.29	14461.2	230.26	79.32	230.07	79.29
Check point 3	31.71	3.29	13719.4	232.86	80.98	232.94	81.56

A checkpoint analysis was performed to confirm the role of the derived polynomial equation and contour plots in predicting the responses.

5.4.3 Formulation optimization by Box-Behnken Design for TBNE

Based on the preliminary investigation, three critical parameters were identified, and their relationship with critical quality attributes (CQA) was exhaustively investigated using Box-Behnken Design. A randomized matrix of 17 runs was generated by Design-Expert software and presented in below table 5.15.

Table 5.15: Randomized BBD design matrix generated Design-Expert software

Run	Independent Variables			Dependent Variables (CQA)	
	A:Oil Concentration (%)	B:Smix Concentration (%)	C:Homogenization Speed (RPM)	Globule size (nm)	%EE
1	40	4	15000	243.33±2.08	76.61±0.53
2	30	2	18000	180.67±1.15	70.55±0.49
3	40	3	12000	270±1.00	77.32±1.22
4	20	2	15000	242±0.63	58.71±1.05
5	40	2	15000	251.33±1.53	76.25±0.49
6	30	4	18000	182±2.00	71.27±0.39
7	30	2	12000	261.99±1.73	69.31±0.44
8	30	4	12000	265.29±0.62	73.49±0.38
9	30	3	15000	237±1.00	80.92±0.34
10	20	3	12000	255.84±1.25	56.62±0.61
11	30	3	15000	240.85±0.78	79.50±0.56
12	30	3	15000	235±1.00	78.29±0.76
13	30	3	15000	246.66±1.53	80.61±0.36
14	20	3	18000	175.17±0.76	59.54±0.51
15	30	3	15000	247.07±1.11	79.65±0.57
16	40	3	18000	199±1.00	78.48±0.50
17	20	4	15000	234.28±2.05	56.27±1.11

5.4.3.1 Effect analysis of critical variables on responses

5.4.3.1.1 Influence of investigated parameters on globule size

A) Statistical Analysis for Globule size

The statistical analysis of the design mentioned above is as follows:

Table 5.16 Statistical analysis of design for Globule size

Source	Sequential p-value	Lack of Fit p-value	Adjusted R^2	Predicted R^2	
Linear	< 0.0001	0.0408	0.8590	0.7878	
2FI	0.9843	0.0217	0.8194	0.5349	
Quadratic	**0.0012**	**0.4291**	**0.9698**	**0.8907**	**Suggested**
Cubic	0.4291		0.9717		**Aliased**

As shown in table 5.16, the best model to fit the experimental results of globule size in nanoemulsion is the quadratic model and was chosen for further evaluation.

B**) ANOVA Analysis for Globule size**

The ANOVA for globule size is given in table 5.17**.**

Table 5.17 ANOVA for Response Surface Quadratic Model for globule size

Source	Sum of Squares	Df	Mean Square	F- value	p-value	
Model	14663.67	9	1629.30	58.06	< 0.0001	Significant
A-Oil Concentration	351.13	1	351.13	12.51	0.0095	
B-Smix Concentration	6.13	1	6.13	0.2182	0.6546	
C-Homogenization Speed	12800.00	1	12800.00	456.10	< 0.0001	
AB	0.2500	1	0.2500	0.0089	0.9274	

AC	25.00	1	25.00	0.8908	0.3767	
BC	0.0000	1	0.0000	0.0000	1.0000	
A^2	18.13	1	18.13	0.6460	0.4480	
B^2	0.7605	1	0.7605	0.0271	0.8739	
C^2	1468.44	1	1468.44	52.32	0.0002	
Residual	196.45	7	28.06			
Lack of Fit	91.25	3	30.42	1.16	0.4291	not significant
Pure Error	105.20	4	26.30			
Cor Total	14860.12	16				

The Model F-value of 58.06 indicates that the model is statistically significant. The probability of such a high F-value occurring by random fluctuation is a mere 0.01%.

P-values below 0.0500 are indicative of significant model terms. In this scenario, the terms A, C, and C^2 have proven to be significant. On the other hand, terms with P-values exceeding 0.1000 are considered insignificant. Eliminating numerous insignificant terms, except those essential for maintaining hierarchical structure, could potentially refine the model.

A Lack of Fit F-value of 1.16 suggests that the lack of fit is not substantial in comparison to pure error, with a 42.91% probability that such a value could result from random noise. A lack of significant fit is favorable as it implies that the model fits well.

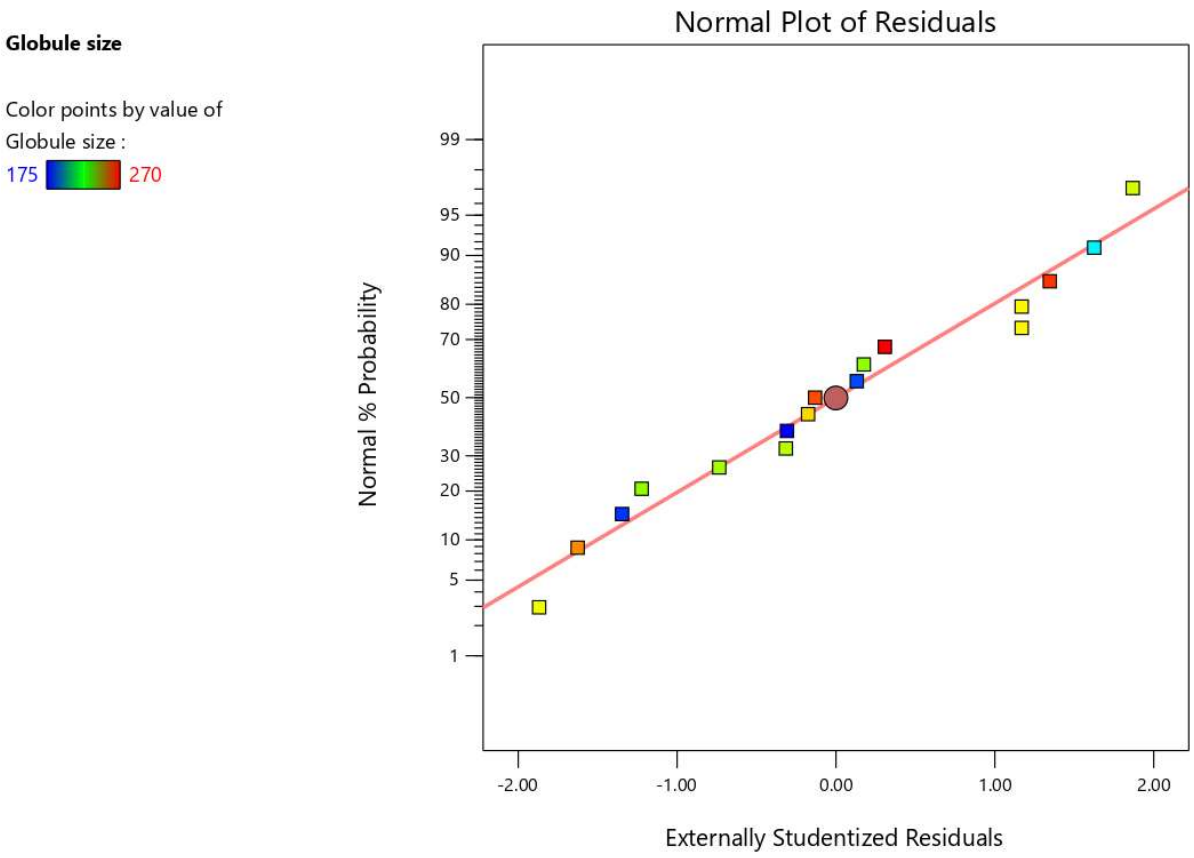

Figure 5.17 Actual v/s Predicted plot for % globule size

Table 5.18 ANOVA study results for globule size

Parameters	Results of Response
Std Deviation	5.30
Mean	233.59
C.V.%	2.27
R-Squared	0.9868
Adjusted R-Squared	0.9698
Predicted R-Squared	0.8907
Adeq. Precision	22.9507

The **Predicted R²** of 0.8907 is in reasonable agreement with the **Adjusted R²** of 0.9698; i.e. the difference is less than 0.2.

Adeq Precision measures the signal to noise ratio. A ratio greater than 4 is desirable. Your ratio of 22.951 indicates an adequate signal. This model can be used to navigate the design space.

C) Mathematical Model for Globule Size

Analyzing the influence of diverse factors on the size of globules, contour and 3D visualizations were utilized alongside ANOVA results. As indicated in table 5.18, variations in factor levels correspond to alterations in the resultant globule size, highlighting the significance of each factor. A detailed examination of these factors reveals the magnitude of their impact. The derived equation delineates the nature of the influence, whether it is augmentative or reductive.

The final equation in terms of coded factors:

Globule size:

$+241.60+6.63*A-0.8750*B+40.00*C+0.2500*AB+2.50*AC+0.0320*BC+2.07*A^2-4250*B^2-18.67*C^2$

Table 5.19 The Final equation in terms of actual factors

Globule Size	=
+241.60	
+6.63	Oil Concentration
-0.8750	S_{mix} Concentration
-40.00	Homogenization speed
+0.2500	Oil Concentration * S_{mix} Concentration
+2.50	Oil Concentration * Homogenization speed
+0.0320	S_{mix} Concentration * Homogenization speed
+2.07	Oil Concentration^2
-4250	S_{mix} Concentration^2
-18.67	Homogenization speed^2

The presence of a positive sign preceding a factor signifies an increase in response with the factor and vice versa. One of the three independent variables that were selected has positive effects on globule size and two of the three independent variables that were selected have

negative effects on globule size as shown by the coefficient values of the individual factors. Moreover, the equation above shows that every component affects globule size to some extent. The equation also reveals that each factor contributes to the variation in globule size. Notably, a higher concentration of oil correlates with an enlargement of globule size. Equation also showed that that with increase in surfactant concentration, there is a decrease in globule size. A higher concentration of surfactant lowers surface tension and aids in globule stabilization. The globule size is negatively impacted by homogenization speed, as the equation illustrates; that is, as homogenization speed increases, globule size decreases. It may be because of the disruption of the globules caused by an increase speed of homogenization (34).

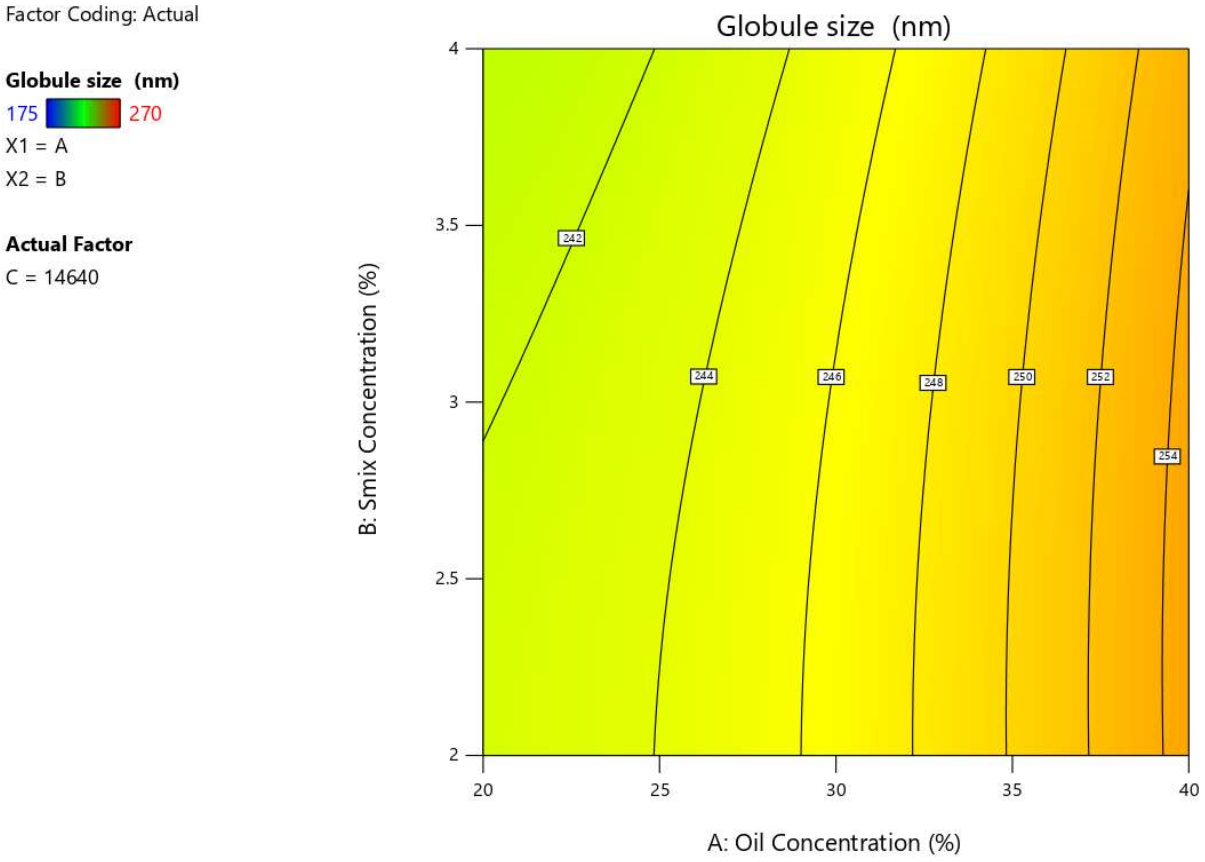

Figure 5.18 Contour plot (2D) showing the combined effect of oil concentration and Smix concentration on globule size

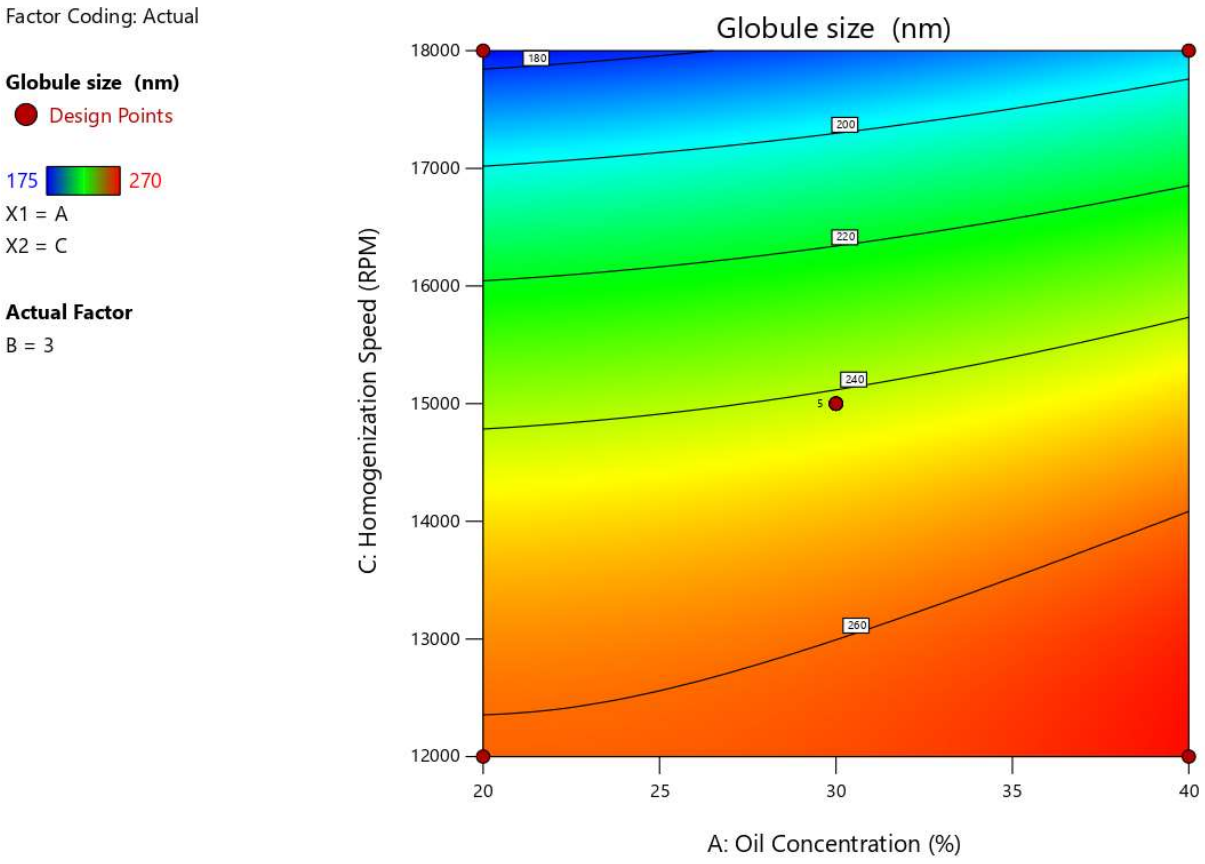

Figure 5.19 Contour plot (2D) showing the combined effect of oil concentration and homogenization speed on globule size

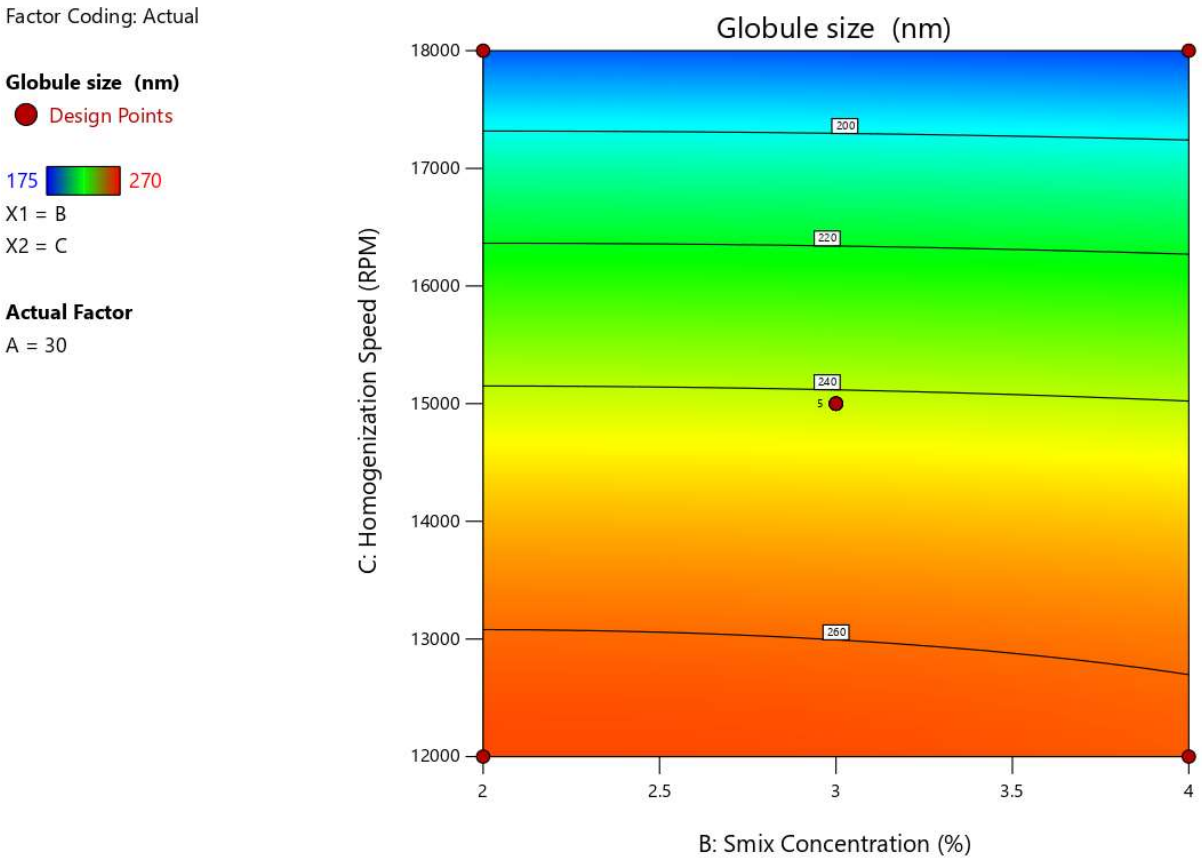

Figure 5.20 Contour plot (2D) showing the combined effect of Homogenization speed and Smix concentration on globule size

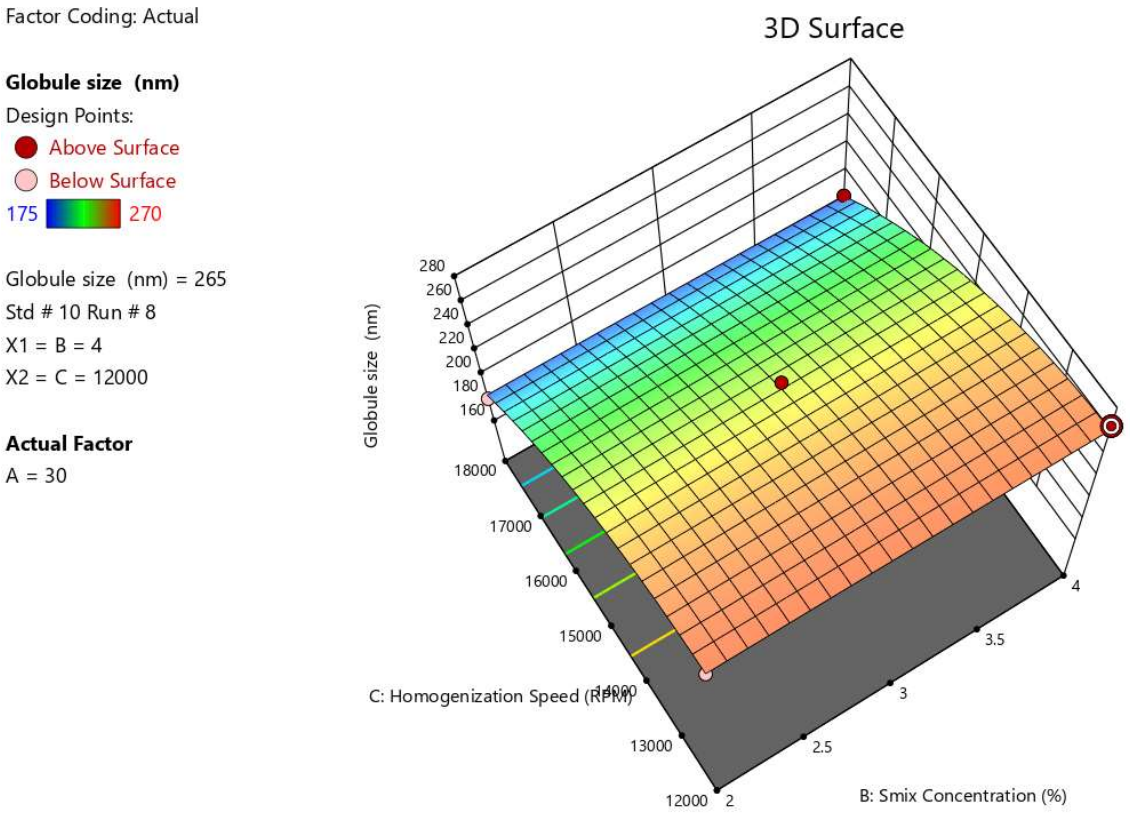

Figure 5.21 Response surface (3D) showing the combined effect of Smix concentration and Homogenization speed on globule size

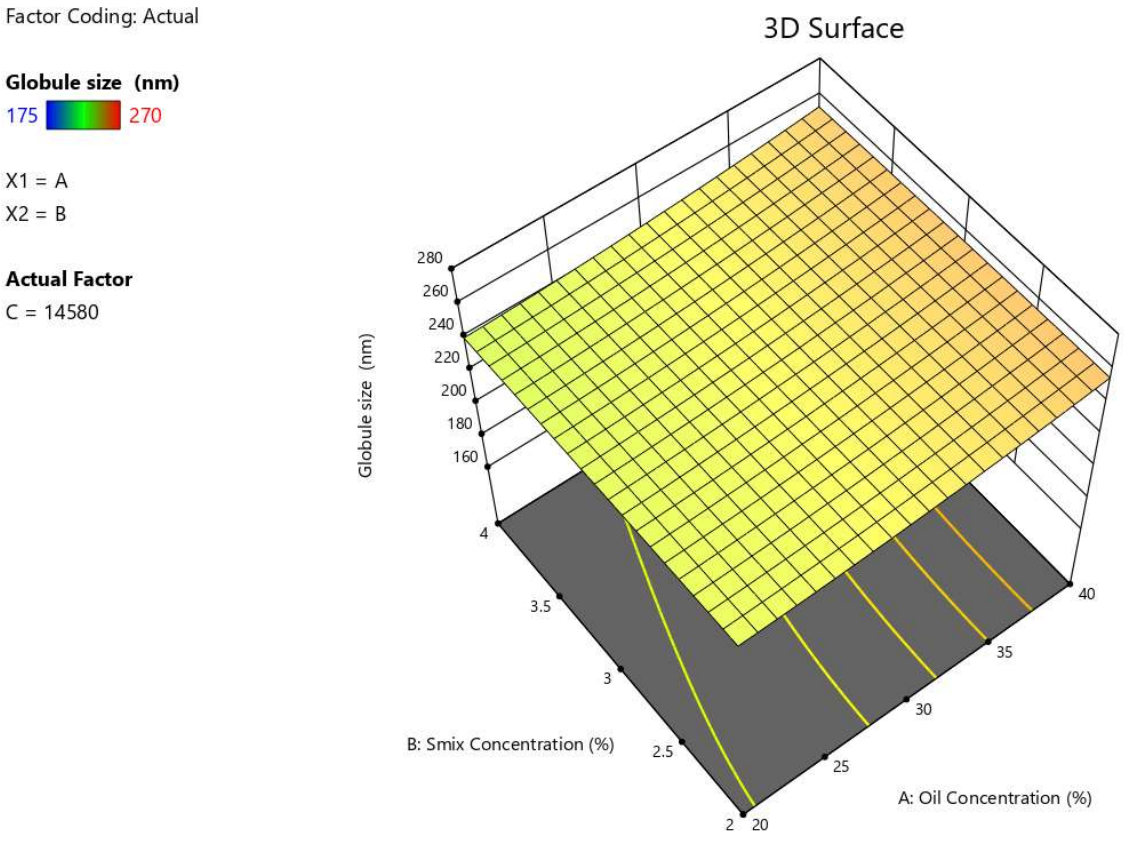

Figure 5.22 Response surface (3D) showing the combined effect of oil concentration and Smix concentration on globule size

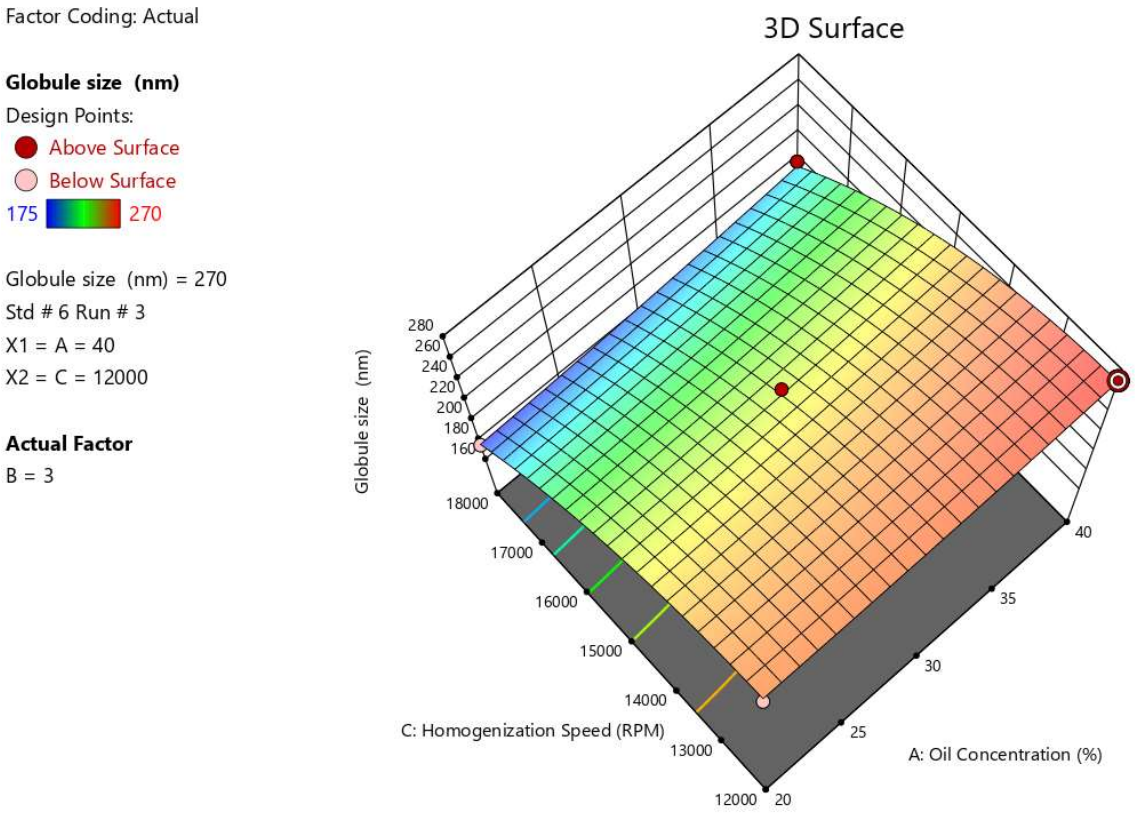

Figure 5.23 Response surface (3D) showing the combined effect of Oil concentration and homogenization speed on globule size

The effects of independent factors on the globule size are shown in Fig. 5.18 to figure 5.23. The highest globule size is shown by the red area, and the lowest globule size is represented by the blue zone. It can be observed that as the S_{mix} concentration increases the globule size increases. As the oil concentration and homogenization speed increases the globule size decreases (34). These graphs show the relationship between the CQA and the corresponding independent factor while maintaining constant levels of the other independent variables.

5.4.3.1.2 Influence of investigated parameters on %EE

A) Statistical Analysis for %EE

The statistical analysis of the design mentioned above is as follows:

Table 5.20 Statistical analysis of design for %EE

Source	Sequential p-value	Lack of Fit p-value	Adjusted R^2	Predicted R^2	
Linear	0.0050	0.0003	0.5256	0.4292	
2FI	0.9949	0.0002	0.3875	0.0145	
Quadratic	**< 0.0001**	**0.1068**	**0.9817**	**0.9007**	**Suggested**
Cubic	0.1068		0.9920		**Aliased**

As shown in table 5.20, the best model to fit the experimental results of %EE in nanoemulsion is the quadratic model and was chosen for further evaluation.

B**) ANOVA Analysis for %EE**

The ANOVA for globule size is given in below table.

Table 5.21 ANOVA for Response Surface Quadratic Model for %EE

Source	Sum of Squares	Df	Mean Square	F- value	p-value	
Model	1232.34	9	136.93	96.29	< 0.0001	Significant
A-Oil Concentration	760.89	1	760.89	535.09	< 0.0001	
B-Smix Concentration	1.58	1	1.58	1.11	0.3263	
C-Homogenization Speed	0.9660	1	0.9660	0.6794	0.4370	
AB	0.4900	1	0.4900	0.3446	0.5756	
AC	0.8100	1	0.8100	0.5696	0.4750	
BC	1.99	1	1.99	1.40	0.2756	
A^2	267.22	1	267.22	187.92	< 0.0001	
B^2	95.06	1	95.06	66.85	< 0.0001	
C^2	60.37	1	60.37	42.45	0.0003	

Residual	9.95	7	1.42			
Lack of Fit	7.47	3	2.49	4.00	0.1068	not significant
Pure Error	2.49	4	0.6218			
Cor Total	1242.29	16				

The significant Model F-value of 96.29 suggests that the model is reliable. The likelihood of such a high F-value arising from random noise is as low as 0.01%. Model terms with P-values below 0.0500 are considered significant, which in this instance includes A, A^2, B^2, and C^2. Conversely, terms with P-values above 0.1000 are deemed insignificant. Eliminating non-essential insignificant terms could potentially enhance the model. Furthermore, the Lack of Fit F-value being 4.00 indicates a non-significant lack of fit when compared to pure error, with a 10.68% probability that such a value could appear by chance. A non-significant lack of fit is desirable as it means the model has a good fit.

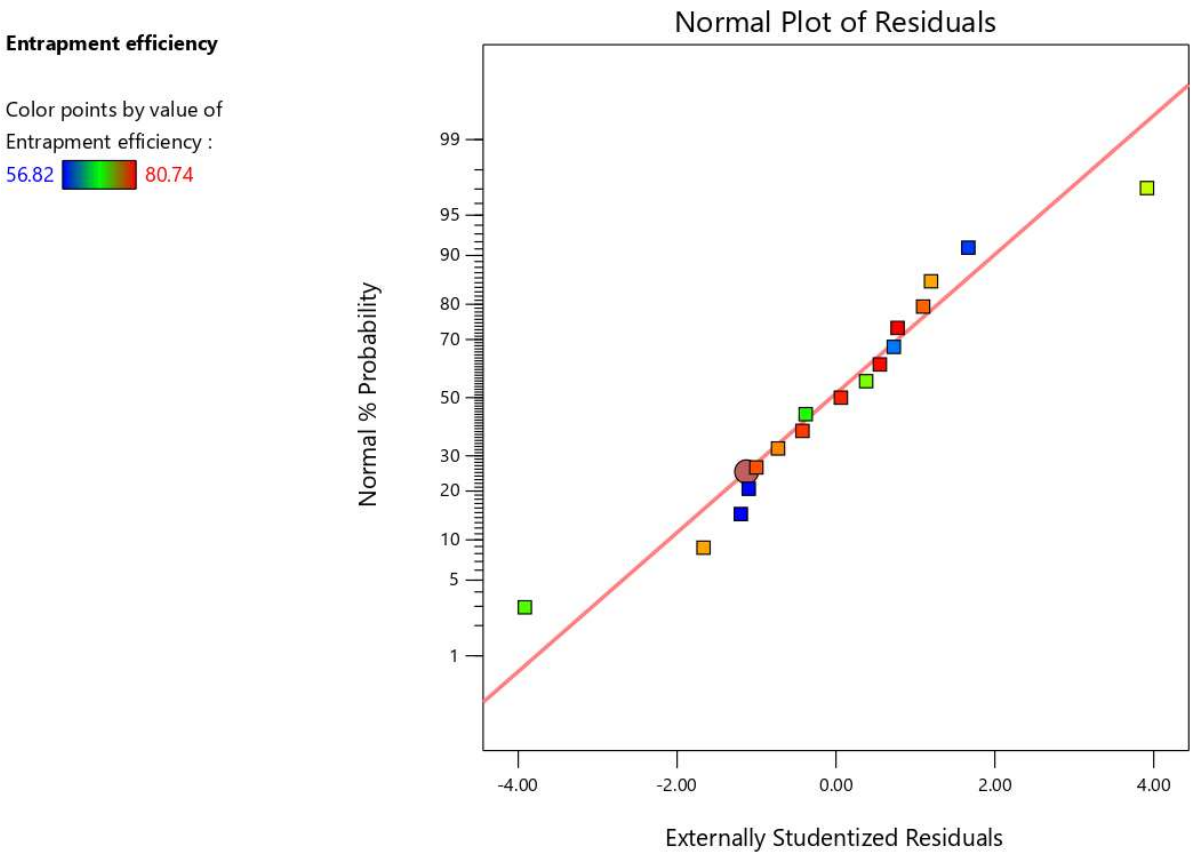

Figure 5.24 Actual v/s Predicted plot for %EE

Table 5.22 ANOVA study results for %EE

Parameters	Results of Response
Std Deviation	1.19
Mean	72.12
C.V.%	1.65
R-Squared	0.9920
Adjusted R-Squared	0.9817
Predicted R-Squared	0.9007
Adeq. Precision	24.6729

The **Predicted R²** of 0.9007 is in reasonable agreement with the **Adjusted R²** of 0.9817; i.e. the difference is less than 0.2.

Adeq Precision measures the signal to noise ratio. A ratio greater than 4 is desirable. Your ratio of 24.673 indicates an adequate signal. This model can be used to navigate the design space.

C) Mathematical Model for %EE

To assess the impact of different factors on %EE, both contour and 3D plots were analyzed, in conjunction with ANOVA values. Table 5.22 illustrates those alterations in factor combinations lead to changes in %EE, thereby verifying the influence of these factors. A detailed investigation of each factor aids in comprehending their impact's scope. The corresponding equation specifies whether the effect is additive or subtractive.

The final equation in terms of coded factors:

%EE: $+79.89+9.75*A+0.4450*B+0.3475*C+0.3500*AB-0.4500*AC-0.7050*BC-7.97*A^2-4.75*B^2-3.79*C^2$

Table 5.23: The Final equation in terms of actual factors

%EE	=
+79.89	
+9.75	Oil Concentration
+0.4450	S_{mix} Concentration
+0.3475	Homogenization speed
+0.3500	Oil Concentration * S_{mix} Concentration
-0.4500	Oil Concentration * Homogenization speed
-0.7050	S_{mix} Concentration * Homogenization speed
-7.97	Oil Concentration^2
-4.75	S_{mix} Concentration^2
-3.79	Homogenization speed^2

The presence of a positive sign preceding a factor signifies an increase in response with the factor and vice versa. Each of the three independent variables that were selected has positive effects on drug entrapment, as shown by the coefficient values of the individual factors. Moreover, the equation above shows that every component affects %EE to some extent. The highest co-efficient value before factor A indicates that oil concentration has the greatest impact on %EE, which is followed by homogenization speed and S_{mix} Concentration. As an example, %EE increases when oil concentration increases. Luliconazole partitioned into the oil phase, resulting in an increase in %EE with an increase in oil concentration. An increase in homogenization speed was shown to cause an increase in %EE. The larger oil globules may break up into numerous fine oil droplets as the stirring speed is increased, trapping as much of the drug as possible in the formulation's oil phase. Increase in Smix concentration also enhances the %EE. This increase could be the result of the drug becoming more soluble in the lipid when the surfactant concentration rises (35).

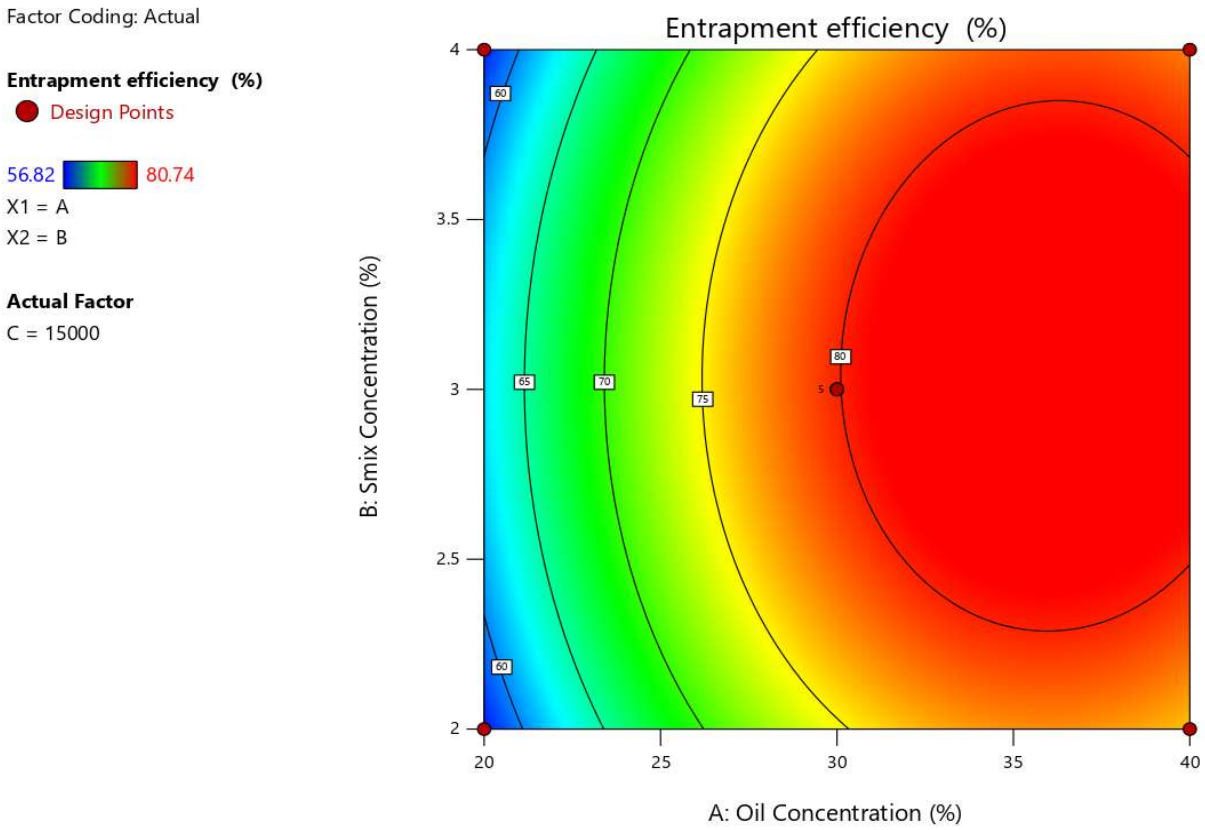

Figure 5.25 Contour plot (2D) showing the combined effect of Oil concentration and Smix Concentration on %EE

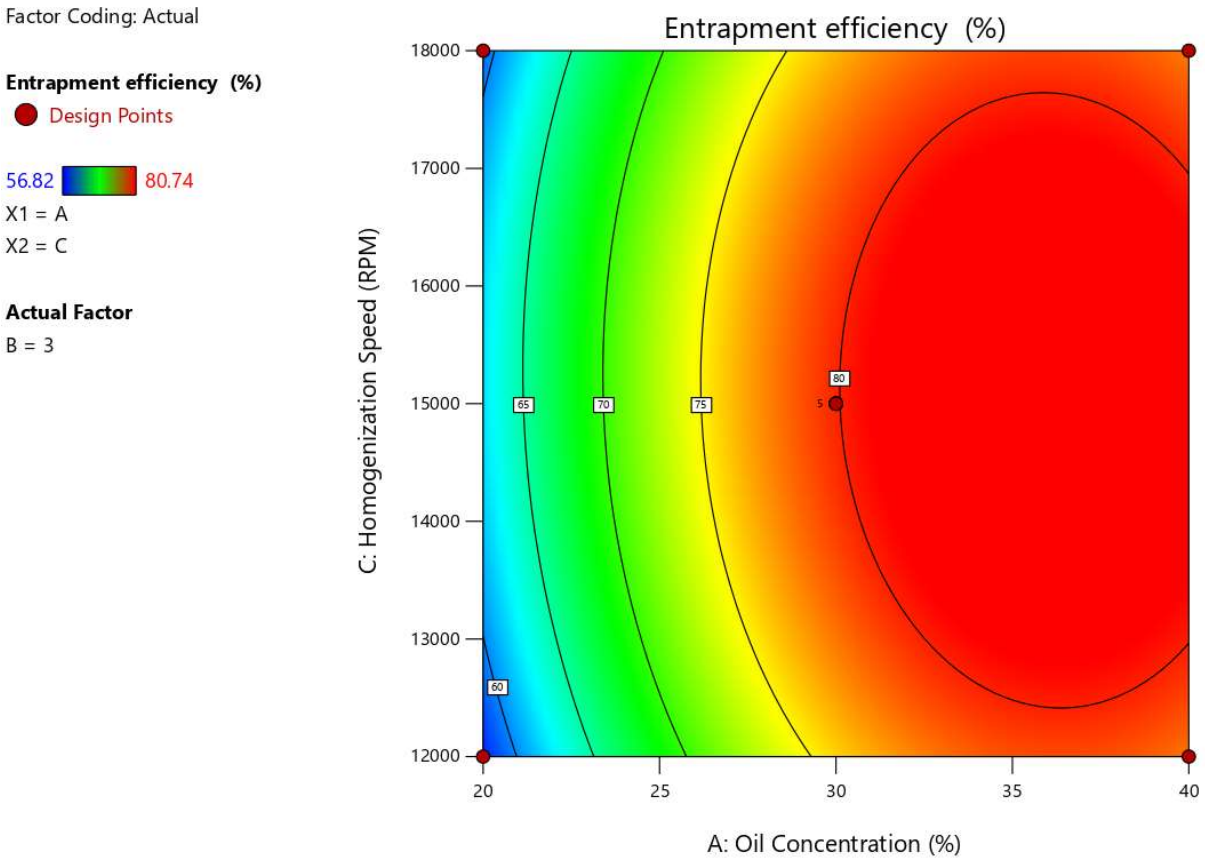

Figure 5.26 Contour plot (2D) showing the combined effect of Oil concentration and Homogenization speed on %EE

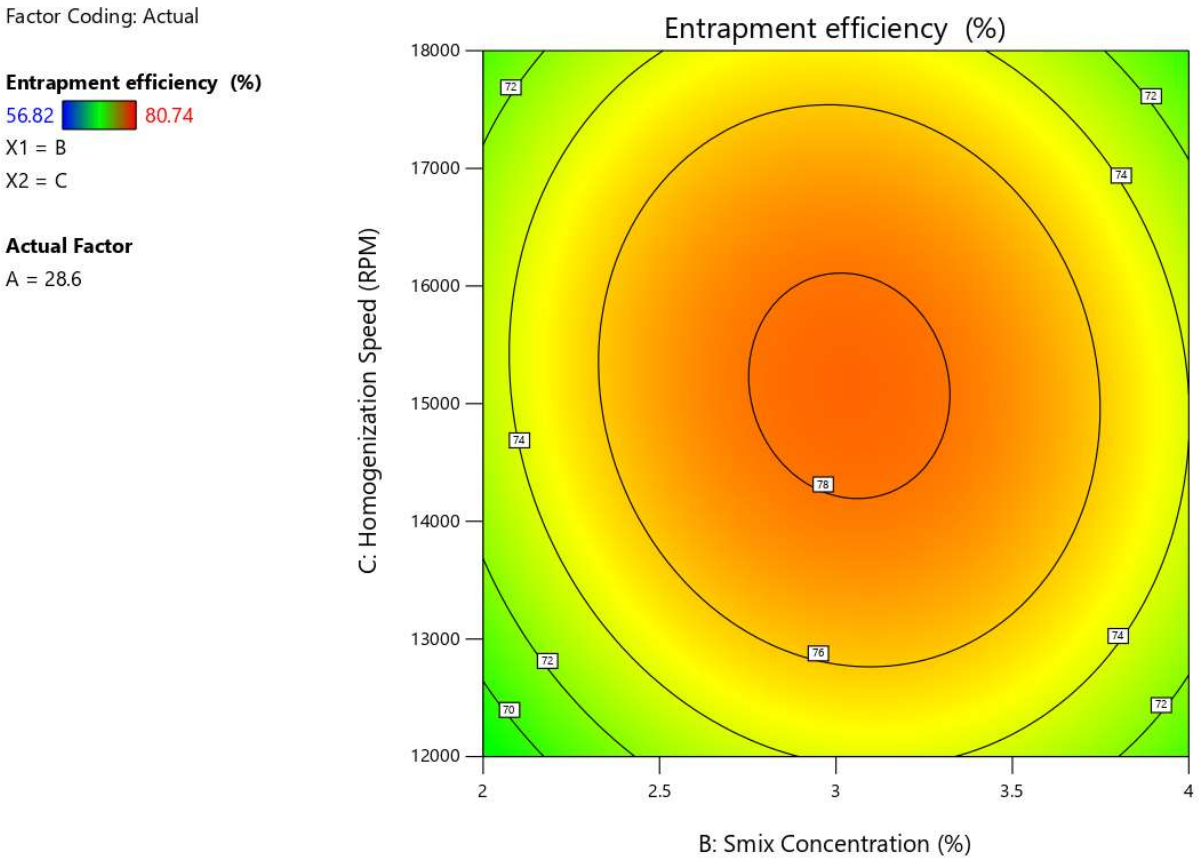

Figure 5.27 Contour plot (2D) showing the combined effect of Smix concentration and Homogenization speed on %EE

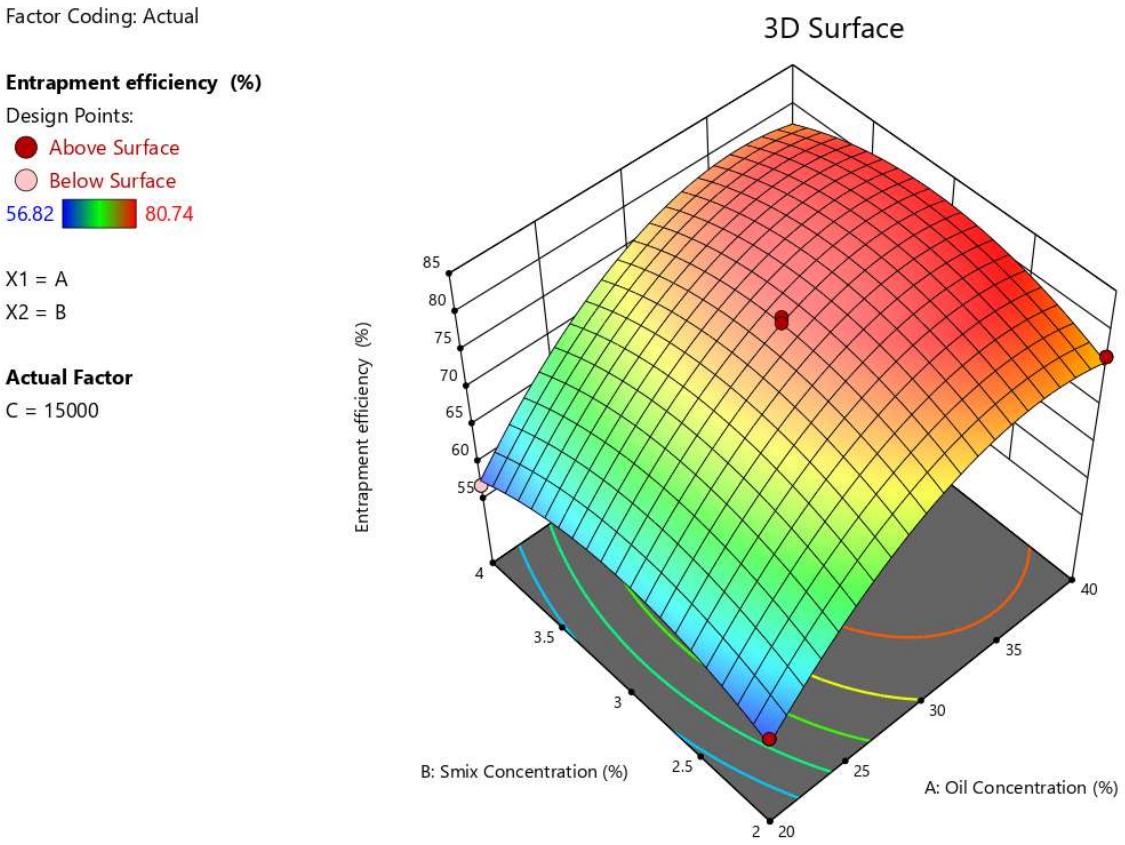

Figure 5.28 Response surface (3D) showing the combined effect of oil concentration and Smix concentration on %EE

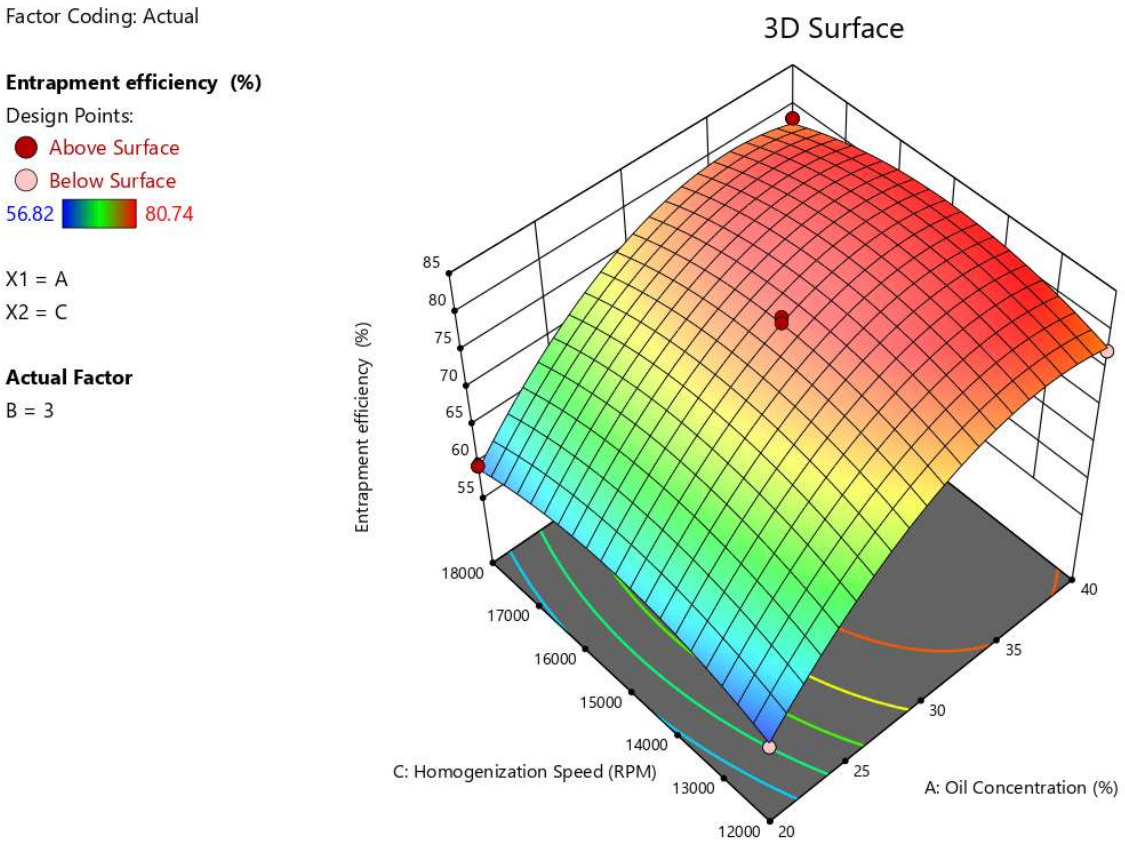

Figure 5.29 Response surface (3D) showing the combined effect of oil concentration and Homogenization speed on %EE

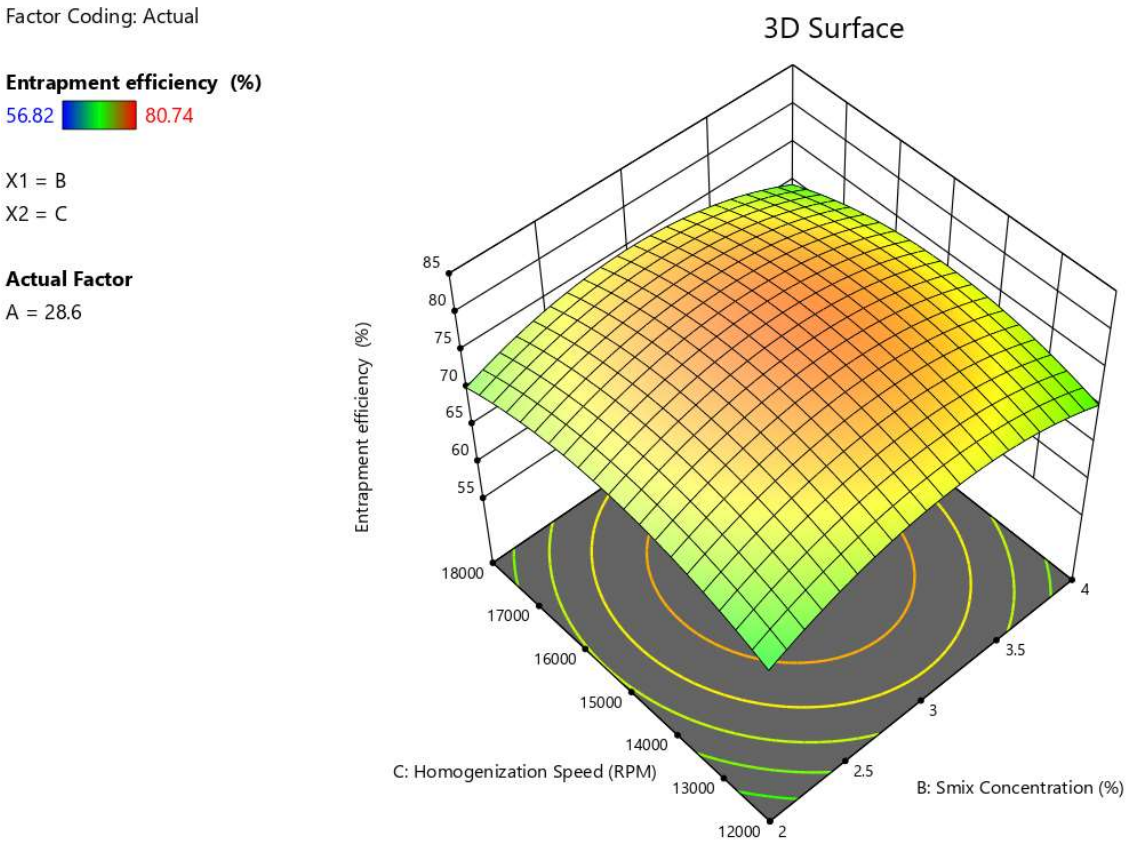

Figure 5.30 Response surface (3D) showing the combined effect of Smix concentration and Homogenization speed on %EE

The effects of independent factors on the %EE are shown in figure 5.25 to figure 5.30. The highest %EE is shown by the red area, and the lowest %EE is represented by the blue zone. These graphs show the relationship between the CQA and the corresponding independent factor while maintaining constant levels of the other independent variables. It is depicted that the drug entrapment increases with increase in the surfactant concentration. The reason for this increase may be an increase in solubility of the drug in the oil on increasing the concentration of the surfactant. However, at higher increment there is reduction in %EE. This may be the result of the drug migrating to these micelles in the emulsion's exterior phase after surfactant micelles form at increasing concentrations (35).

5.4.3.2 Preparation of checkpoint batches as per the overlay plot

Overlay contour plots for all two CQAs (%EE and globule size) were generated (Fig. 5.31) for obtaining the design space (yellow area in graph).

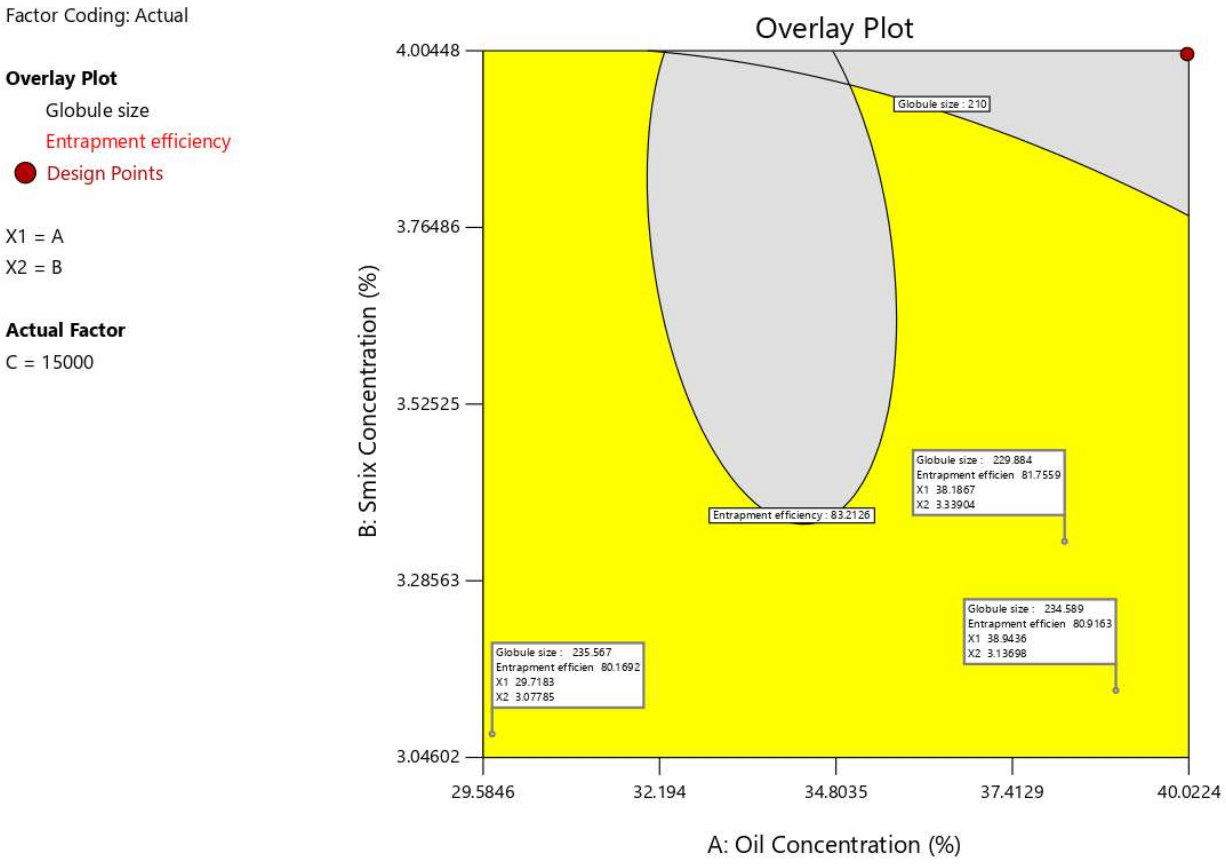

Figure 5.31 Overlay plot of TBNE

Table 5.24: Results of check point batches for globule size and %EE

Batch	X1 (%Oil Concentration)	X2 (%S_{mix} Concentration)	X3 Homogenization speed)	Y1 (Globule Size)	Y2 (%EE)	Predicated Y1 (Globule Size)	Predicated Y2 (%EE)
Check point 1	38.19	3.34	15000	229.08	81.53	229.88	81.76
Check point 2	29.72	3.08	15000	235.12	80.43	235.57	80.17

Check point 3	38.94	3.14	15000	233.91	80.45	234.59	80.92

A checkpoint analysis was performed to confirm the role of the derived polynomial equation and contour plots in predicting the responses.

Table 5.25: Composition of optimized batch of LZNE loaded gel and TBNE loaded gel

Formulation components	LZNE loaded gel (100 gm)	TBNE loaded gel (100 gm)
API	1 gm LZ	5 gm TB
Capmul MCM C8	21 gm	21 gm
Coconut oil	9 gm	9 gm
Cremophore EL	2 gm	2 gm
Pluronic F127	1 gm	1 gm
Water	61 gm	57 gm
Homogenization speed	15000	15000
Sonication	80 watts, 2 cycles of one min each	80 watts, 2 cycles of one min each
Carbopol 974 P	1 gm	1 gm
Propylene Glycol	4 gm	4 gm
Triethanolamine	pH adjuster	pH adjuster

5.4.4 Characterization of LZNE and TBNE

5.4.4.1 Globule size, PDI, Zeta Potential and %EE

Globule size of the optimized formulation of LZ NE and TB NE were found to be 237.26±0.35 nm and 234.32±0.81 nm respectively. The zeta potential measurements for the LZNE and TBNE were -28.54±0.94 and -26.12±1.32, respectively. The zeta potential of a nanoemulsion is a measure of the charge on its globules. It indicates the degree of repulsion between globules with the same charge. Surface of particles in suspension develops a charge due to adsorption of ions or ionisation of surface group and the charge is correspondingly dependent on both the surface chemistry and the environment of particles. Same way emulsion also develops charges due to the layer of surfactant around the globules. The surface charge generates a potential around the

globules, which is high near the surface and decays with distance into the dispersion medium (13). A higher zeta potential value (>±30 mV) indicates a more stable nanoemulsion. This is because the repulsion between particles prevents them from aggregating. A lower zeta potential value (< 15 mV) indicates a less stable nanoemulsion, where flocculation is more likely to occur (36). The zeta potential of the formulation was found to be slightly negative in spite of the non-ionic nature of the surfactant, co-surfactant and the oil. This indicated that the formulation would remain physically stable on storage (37). Polydispersity Index (PDI) values were recorded at 0.182±0.04 for LZNE and 0.202±0.06 for TBNE. The PDI value of developed nanoemulsions is below 0.3 which shows low polydispersity and acceptable level of homogeneity of developed formulations (38). Furthermore, the entrapment efficiencies were determined to be 80.28±1.14% for LZNE and 79.82±0.72% for TBNE. Solubility of drug in oil phase and optimum concentration of S_{mix} are probable reasons for the higher %EE of the developed formulations.

5.4.4.2 Centrifugal stability test

To assess the physical stability of the nanoemulsion, it was subjected to centrifugation at speeds ranging from 4000 to 10,000 rpm, each for duration of 20 minutes. The formulation was then examined for any signs of phase separation. After 15 days, a slight alteration in globule size was noted when centrifuged between 4000 and 8000 rpm for 20 minutes each. However, the freshly prepared nanoemulsion exhibited stability with no observable instability at speeds up to 8000 rpm.

5.4.4.3 Transmittance

The clarity of the optimized LZNE and TBNE was quantified using a UV spectrophotometer (UV 1900, Shimadzu, Japan) at a wavelength of 630 nm. The transmittance values for LZNE and TBNE were recorded at 98.34±0.21% and 99.16±0.11% respectively. %Transmittance closer to 100% indicates that the optimized formulations were clear, transparent and able to transmit light (39).

5.4.4.4 Differential scanning Calorimetry (DSC)

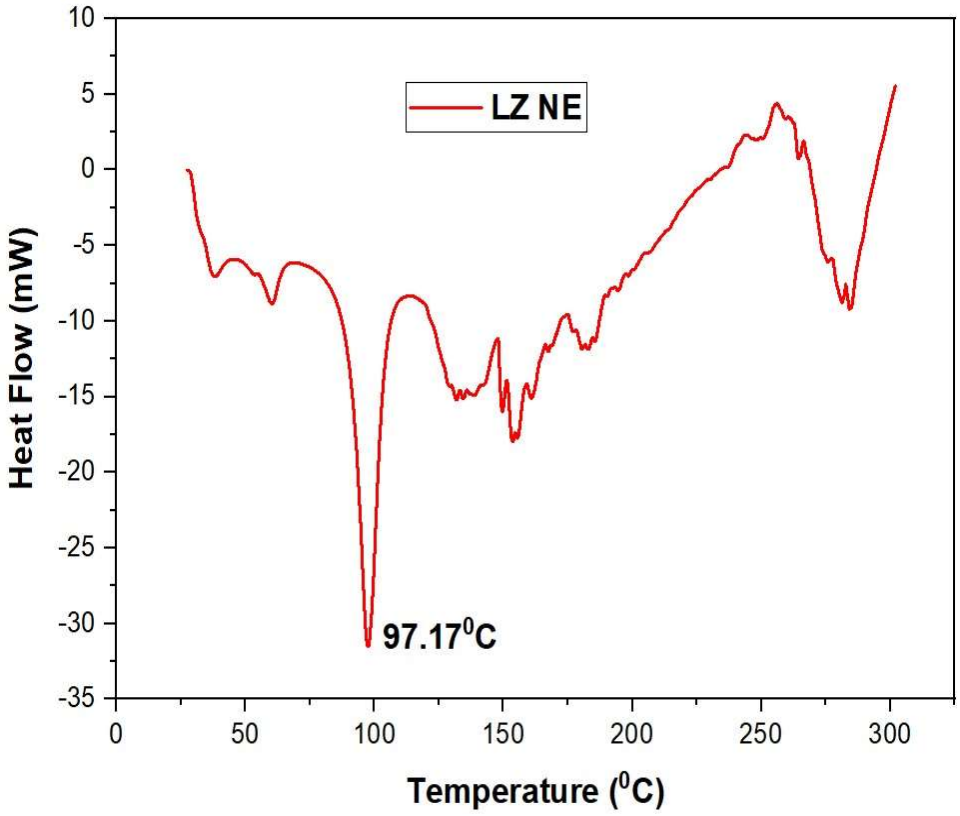

Figure 5.32: DSC graph of LZNE

Figure 5.32 showed the DSC graph of Luliconazole loaded NE. It showed the absence of the endothermic drug peak (melting point of Luliconazole 157.89°C – mentioned in figure 4.14 of chapter 4) which indicated no crystalline nature of the drug in the developed formulation.

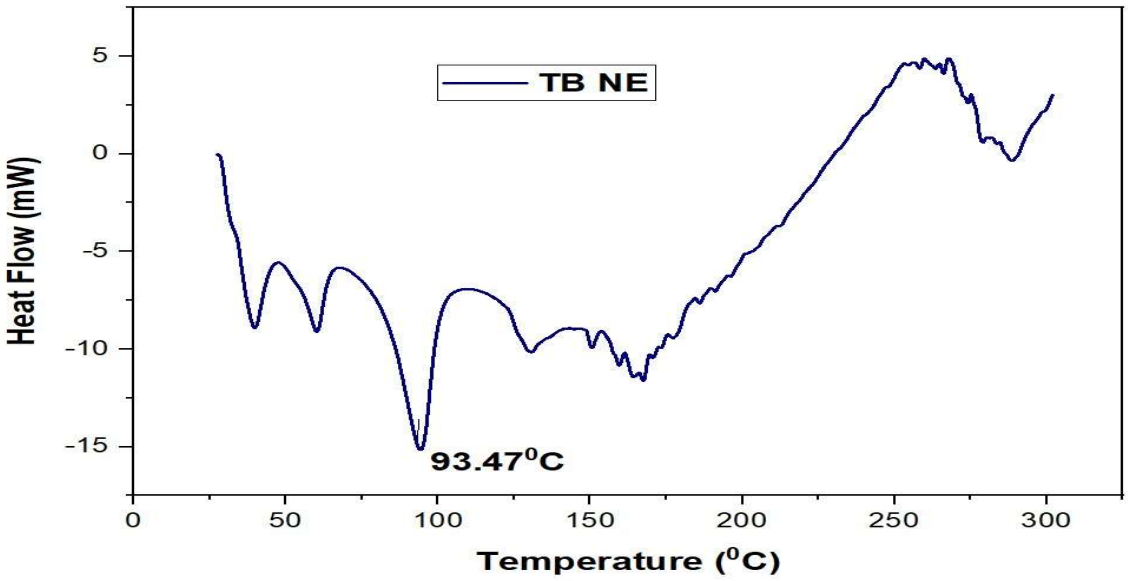

Figure 5.33: DSC graph of TBNE

Figure 5.33 showed the DSC graph of Tavaborole loaded NLCs. It showed the absence of the endothermic drug peak (melting point of Tavaborole 116.16 °C – mentioned in figure 4.15 of chapter 4) which indicated no crystalline nature of the drug in the developed formulation.

5.4.4.5 Transmission electron microscopy (TEM)

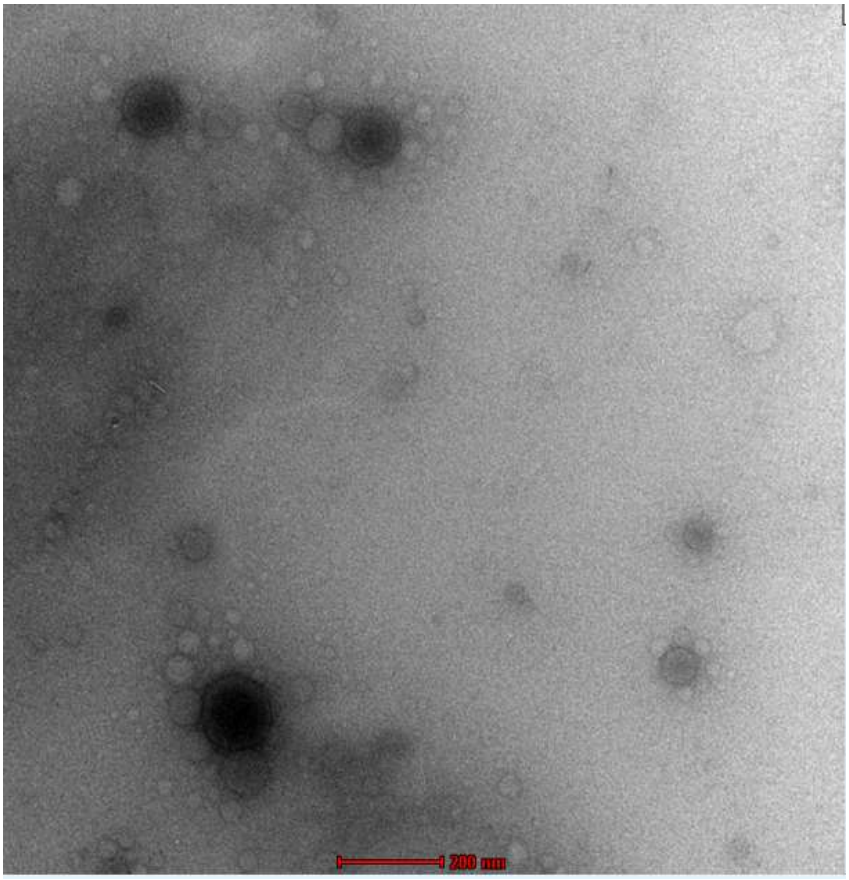

Figure 5.34 TEM image of LZNE

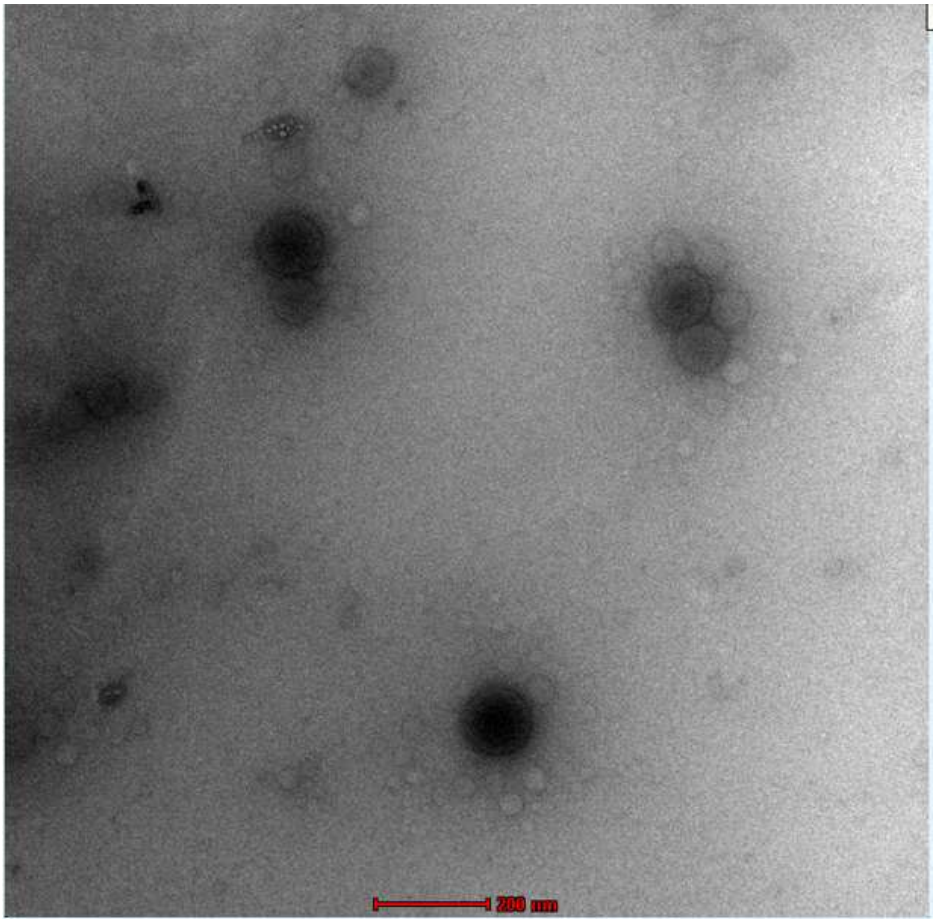

Figure 5.35 TEM image of TBNE

Figure 5.34 and figure 5.35 showed TEM images of LZNE and TBNE. The images demonstrated spherical shapes of the nanoemulsion droplets. TEM analysis also confirmed the nanometric droplet diameter of developed formulations.

5.4.4.6 Powder X-ray diffraction studies

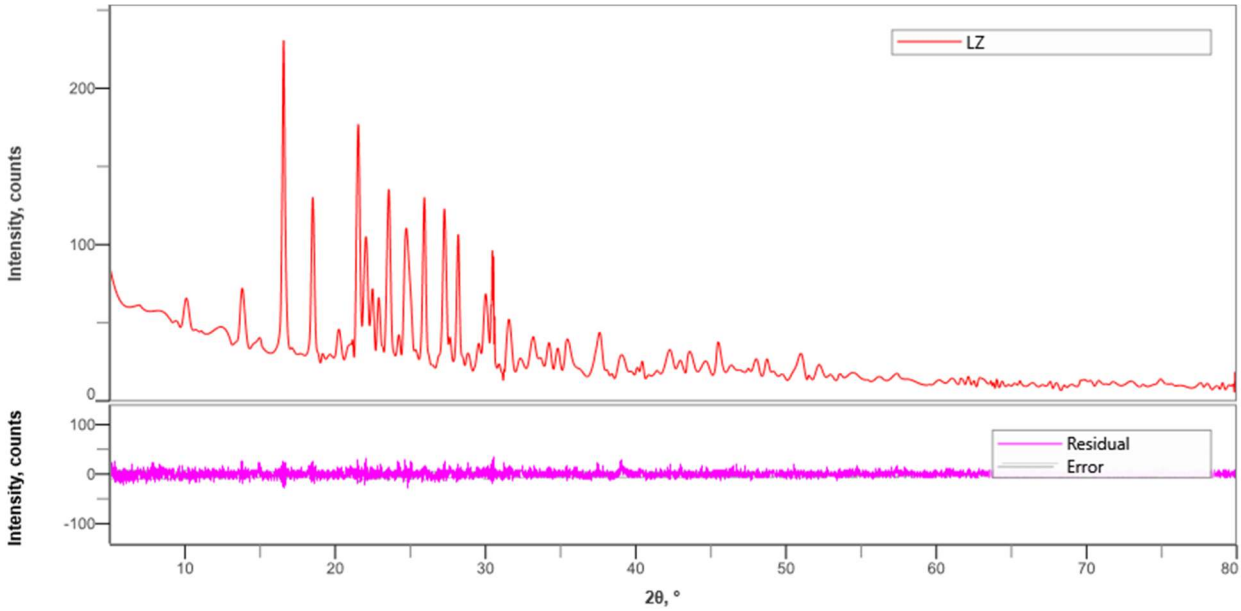

Figure 5.36: XRD of Luliconazole

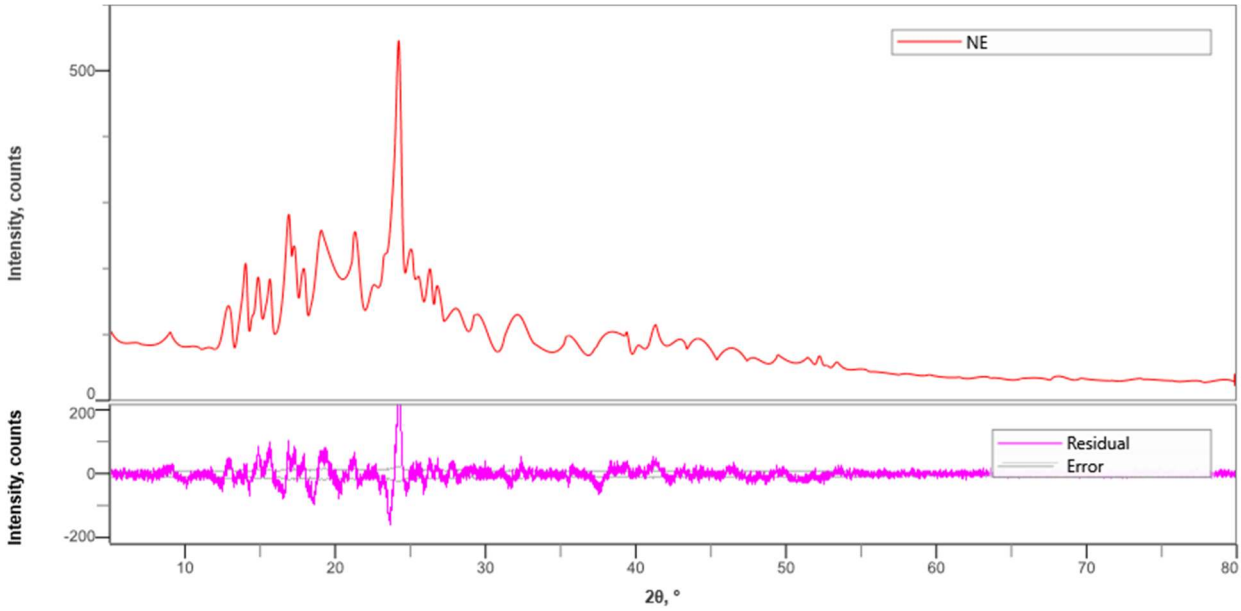

Figure 5.37: XRD graph of LZNE

As shown in figure 5.36 Luliconazole showed intense peaks because of its crystalline structure. Figure 5.37 shows diffraction patterns of nanoemulsion confirmed the transformation of drug from crystalline state to amorphous state in Nanoemulsion.

5.4.5 Characterization of optimized Luliconazole and Tavaborole nanoemulsion based gel

5.4.5.1 Viscosity of gel

Viscosity measurements indicated that Luliconazole nanoemulsion gel (1305 ± 0.362 cPs) had a higher viscosity than its free gel counterpart (1172 ± 0.256 cPs), suggesting enhanced skin adherence for the nanoemulsion formulation. Similarly, Tavaborole nanoemulsion gel (1831 ± 0.291 cPs) exhibited increased viscosity compared to the free gel (1543 ± 0.543 cps), implying improved retention on the skin.

5.4.5.2 Spreadability of gel

The spreadability of gel preparations is defined as the ability of the gel to be spread on the surface of the skin. Good spreadability can guarantee the better distribution of a gel when applied to the skin (40). The spreadability of free Luliconazole gel and LZNE based gel was found to be 11.21 ± 1.54 gm.cm/sec and 15.23 ± 1.28 gm.cm/sec, respectively, demonstrates the good spreadability of the formulated gel. The spreadability of free Tavaborole gel and TBNE based gel was found to be 9.38 ± 1.02 gm.cm/sec and 14.67 ± 2.31 gm.cm/sec, respectively, demonstrates the good spreadability of the formulated gel.

5.4.5.3 pH of gel

The pH of free Luliconazole gel and Luliconazole nanoemulsion based gel was found to be 6.0±0.12 and 6.3±0.3, respectively, which aligns with skin pH to minimize irritation.

The pH of free Tavaborole gel and Tavaborole nanoemulsion based gel was found to be 5.9±0.48 and 6.1±0.19, respectively, which aligns with skin pH to minimize irritation.

5.4.5.4 Assay of gel

Drug content analysis revealed that Luliconazole and Tavaborole were present at 97.31 ± 0.41% (9.73 mg/gm) and 97.77 ± 0.51% (48.89 mg/gm) in their respective nanoemulsion-based gels which is equivalent to marketed formulations (41).

5.4.5.5 Gel Strength

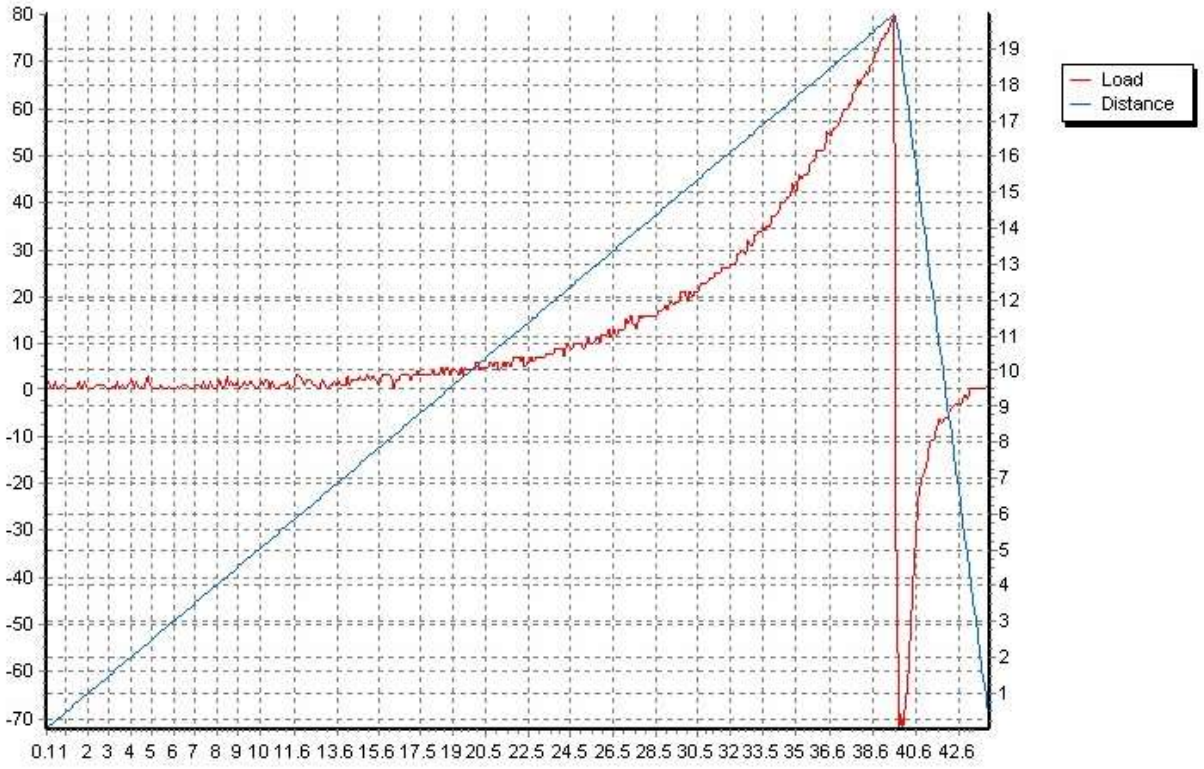

Figure 5.38: Gel strength of LZNE

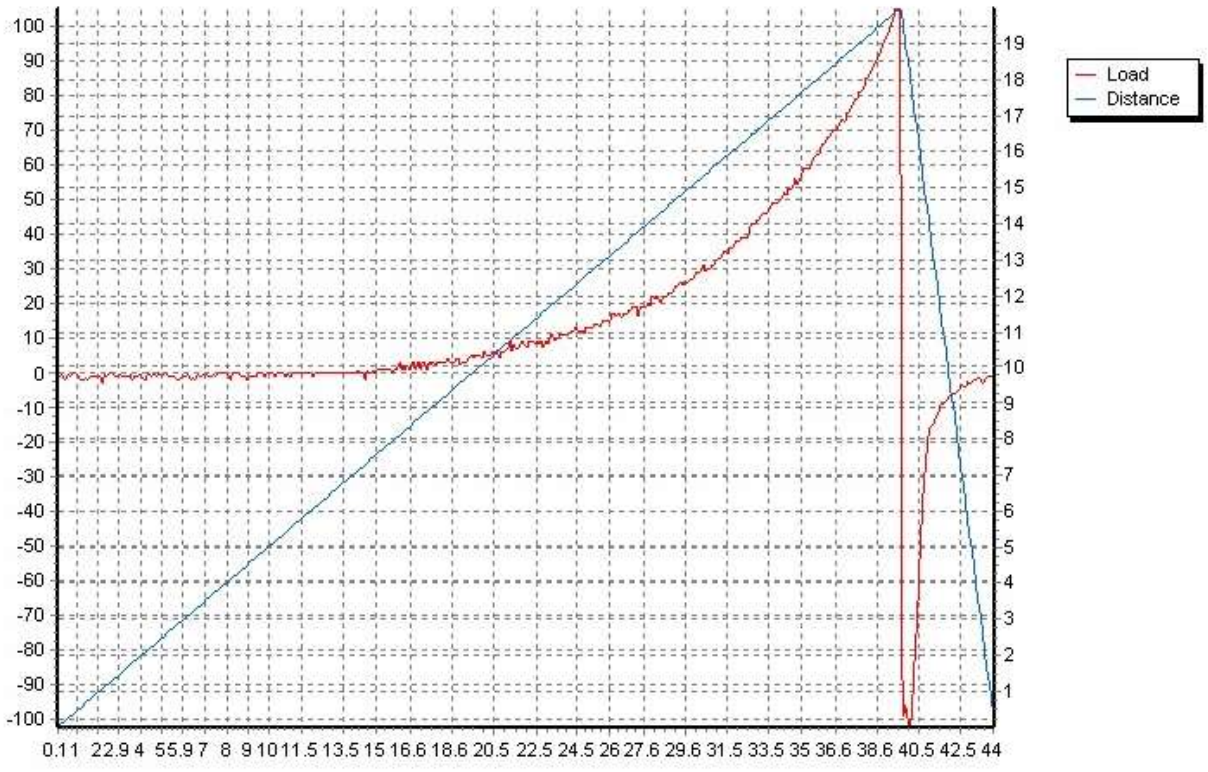

Figure 5.39: Gel strength of TBNE

Gel strength is a measure of a colloidal dispersion's capacity to form and sustain a gel form. Strong gels will withstand far greater pressure than weak gels before being flushed from the site of administration, and it will affect the spreadability and drug's release. This makes gel strength crucial (42). Figure 5.38 and figure 5.39 indicated gel strength of LZNE and TBNE 80 gm and 102 gm respectively. Graphs indicate that both gels have significant gel strength.

5.5 References

1. Eqbal, Asif, et al. "Recent applications of nanoemulsion based drug delivery system: A review." *Research journal of pharmacy and technology* 14.5 (2021): 2852-2858.
2. Choudhury, Hira, et al. "Recent update on nanoemulsion based gel as topical drug delivery system." *Journal of pharmaceutical sciences* 106.7 (2017): 1736-1751.
3. Salim, Norazlinaliza, et al. "Nanoemulsion as a topical delivery system of antipsoriatic drugs." *RSC advances* 6.8 (2016): 6234-6250.
4. Abdulbaqi, Mustafa R., and N. A. Rajab. "Apixaban ultrafine O/W nano emulsion transdermal drug delivery system: formulation, in vitro and ex vivo characterization." *Syst. rev. pharm* 11 (2020): 82-94.
5. Fernández-Campos, F., et al. "Evaluation of novel nystatin nanoemulsion for skin candidosis infections." *Mycoses* 56.1 (2013): 70-81.
6. Shaikh, Neha M., et al. "Formulation and evaluation of nanoemulsion for topical application." *Journal of drug delivery and therapeutics* 9.4-s (2019): 370-375.
7. Kumar, Sushil, et al. "Design and development of ciclopirox topical nanoemulsion gel for the treatment of subungual onychomycosis." *Indian journal of pharmaceutical education and research* 46.4 (2012): 303-311.
8. Yadav, Umesh, et al. "Development, optimization and characterization of topical nanoemulsion gel of an antifungual agent for effective treatment of onychomycosis." *Pharma research library* 2 (2015): 25-36.
9. Mahtab, Asiya, et al. "Transungual delivery of ketoconazole nanoemulsion based gel for the effective management of onychomycosis." *AAPS pharmSciTech* 17 (2016): 1477-1490.
10. Gul, Uzma, et al. "Olive oil and clove oil-based nanoemulsion for topical delivery of terbinafine hydrochloride: in vitro and ex vivo evaluation." *Drug delivery* 29.1 (2022): 600-612.
11. Negi, Poonam, et al. "Biocompatible lidocaine and prilocaine loaded-nanoemulsion system for enhanced percutaneous absorption: QbD-based optimisation, dermatokinetics and in vivo evaluation." *Journal of microencapsulation* 32.5 (2015): 419-431.

12. Knopp, Matthias Manne, et al. "Comparative study of different methods for the prediction of drug–polymer solubility." *Molecular pharmaceutics* 12.9 (2015): 3408-3419.
13. Thakkar, Hetal P., et al. "Formulation and evaluation of Itraconazole nanoemulsion for enhanced oral bioavailability." *Journal of microencapsulation* 32.6 (2015): 559-569.
14. Aqil, Mohd, et al. "Development of clove oil based nanoemulsion of olmesartan for transdermal delivery: Box–Behnken design optimization and pharmacokinetic evaluation." *Journal of molecular liquids* 214 (2016): 238-248.
15. Poonia, Neelam, et al. "Optimization and Development of Methotrexate-and Resveratrol-Loaded Nanoemulsion Formulation Using Box–Behnken Design for Rheumatoid Arthritis." *Assay and drug development technologies* 18.8 (2020): 356-368.
16. Chaudhari, Pallavi M., And Madhavi A. Kuchekar. "Development and evaluation of nanoemulsion as a carrier for topical delivery system by box-behnken design." *Development* 11.8 (2018).
17. Rachmawati, Heni, et al. "In vitro study on antihypertensive and antihypercholesterolemic effects of a curcumin nanoemulsion." *Scientia pharmaceutica* 84.1 (2016): 131.
18. Carpenter, Jitendra, and Virendra Kumar Saharan. "Ultrasonic assisted formation and stability of mustard oil in water nanoemulsion: Effect of process parameters and their optimization." *Ultrasonics sonochemistry* 35 (2017): 422-430.
19. Deeksha, K., and Sowmya Hari. "Synthesis, Characterization and Antibacterial effect of Neem Oil Nanoemulsion." *Research journal of pharmacy and technology* 12.9 (2019): 4400-4404.
20. Cong, Zhaotong, et al. "Design and optimization of thermosensitive nanoemulsion hydrogel for sustained-release of praziquantel." *Drug development and industrial pharmacy* 43.4 (2017): 558-573.
21. Singh, Sangeeta, Tarun Virmani, and Kanchan Kohli. "Nanoemulsion system for improvement of raspberry ketone oral bioavailability." *Indo glob. J. pharm. Sci* 10.01 (2020): 33-42.

22. Chaudhari, Mansi J., et al. "Application of area under curve technique for UV-Spectrophotometric determination of Luliconazole in bulk and pharmaceutical formulation." *Asian journal of pharmaceutical analysis* 8.1 (2018): 45-48.
23. Thakkar, Hetal P., et al. "Formulation and evaluation of Itraconazole nanoemulsion for enhanced oral bioavailability." *Journal of microencapsulation* 32.6 (2015): 559-569.
24. Passos, Julia Sapienza, et al. "Development, skin targeting and antifungal efficacy of topical lipid nanoparticles containing itraconazole." *European journal of pharmaceutical sciences* 149 (2020): 105296.
25. Salvia-Trujillo, Laura, et al. "Effect of processing parameters on physicochemical characteristics of microfluidized lemongrass essential oil-alginate nanoemulsions." *Food hydrocolloids* 30.1 (2013): 401-407.
26. Kurniawansyah, Insan Sunan, Iyan Sopyan, And Geni Refsi. "Physical Characterization of In Situ Ophthalmic Gel: A Concise Review." *Int J App Pharm* 14.1 (2022): 18-21.
27. Bonacucina, Giulia, Sante Martelli, and Giovanni F. Palmieri. "Rheological, mucoadhesive and release properties of Carbopol gels in hydrophilic cosolvents." *International journal of pharmaceutics* 282.1-2 (2004): 115-130.
28. Xing, Lei, et al. "pH-sensitive and specific ligand-conjugated chitosan nanogels for efficient drug delivery." *International journal of biological macromolecules* 141 (2019): 85-97.
29. Nasirpour-Tabrizi, Parisa, et al. "Production of a spreadable emulsion gel using flaxseed oil in a matrix of hydrocolloids." *Journal of food processing and preservation* 44.8 (2020): e14588.
30. Mulia, Kamarza, Rosalia MA Ramadhan, and Elsa A. Krisanti. "Formulation and characterization of nanoemulsion based gel mangosteen extract in virgin coconut oil for topical formulation." *MATEC web of conferences*. Vol. 156. EDP Sciences, 2018.
31. Nagaraja, Sreeharsha, et al. "Topical nanoemulsion based gel for the treatment of skin cancer: Proof-of-technology." *Pharmaceutics* 13.6 (2021): 902.
32. Morsy, Mohamed A., et al. "Preparation and evaluation of atorvastatin-loaded nanoemulgel on wound-healing efficacy." *Pharmaceutics* 11.11 (2019): 609.
33. Doshi, Akashkumar, Bala Prabhakar, and Sarika Wairkar. "Prolonged retention of luliconazole nanofibers for topical mycotic condition: development, in vitro

characterization and antifungal activity against Candida albicans." *Journal of materials science: materials in medicine* 35.1 (2024): 46.

34. Tang SY, Shridharan P, Sivakumar M. Impact of process parameters in the generation of novel aspirin nanoemulsions – Comparative studies between ultrasound cavitation and microfluidizer. *Ultrason sonochem*, 2013;20(1):485–97.
35. Jadhav, Shital Tanaji, Vijay Rajaram Salunkhe, and Somnath Devidas Bhinge. "Nanoemulsion drug delivery system loaded with imiquimod: a QbD-based strategy for augmenting anti-cancer effects." *Future journal of pharmaceutical sciences* 9.1 (2023): 120.
36. Gurpreet, K., and S. K. Singh. "Review of nanoemulsion formulation and characterization techniques." *Indian journal of pharmaceutical sciences* 80.5 (2018).
37. Thakkar, Hetal, et al. "Formulation and characterization of lipid-based drug delivery system of raloxifene-microemulsion and self-microemulsifying drug delivery system." *Journal of pharmacy and bioallied sciences* 3.3 (2011): 442-448.
38. Eid, Ahmad Mustafa Masoud, N. A. Elmarzugi, and Hesham Ali El-Enshasy. "Preparation and evaluation of olive oil nanoemulsion using sucrose monoester." *Int J Pharm pharm sci* 5.Suppl 3 (2013): 434-440.
39. Laxmi, Moksha, et al. "Development and characterization of nanoemulsion as carrier for the enhancement of bioavailability of artemether." *Artificial cells, nanomedicine, and biotechnology* 43.5 (2015): 334-344.
40. Nurman, Salfauqi, et al. "The optimization of gel preparations using the active compounds of arabica coffee ground nanoparticles." *Scientia pharmaceutica* 87.4 (2019): 32.
41. Shaikh, Mohd Sayeed, et al. "Development and validation of UV spectrophotometric method for the estimation of luliconazole in bulk, marketed formulations." *Journal of current pharma research* 10.3 (2020): 3759-3770.
42. Ullah, Kamran Hidayat, et al. "Poloxamer 407 based gel formulations for transungual delivery of hydrophobic drugs: Selection and optimization of potential additives." *Polymers* 13.19 (2021): 3376.